

Design, evaluation and future projections of the NARClIM 2.0 CORDEX-CMIP6 Australasia regional climate ensemble

Giovanni Di Virgilio^{1,2}, Jason P. Evans^{2,3}, Fei Ji^{1,3}, Eugene Tam¹, Jatin Kala⁴, Julia Andrys⁴, Christopher Thomas², Dipayan Choudhury¹, Carlos Rocha¹, Stephen White¹, Yue Li¹, Moutassem El Rafei¹, Rishav Goyal¹, Matthew L. Riley¹ and Jyothi Lingala⁴

¹Climate & Atmospheric Science, NSW Department of Climate Change, Energy, the Environment and Water, Sydney, Australia

²Climate Change Research Centre, University of New South Wales, Sydney, Australia

³Australian Research Council Centre of Excellence for Climate Extremes, University of New South Wales, Sydney, Australia

⁴Environmental and Conservation Sciences, and Centre for Climate Impacted Terrestrial Ecosystems, Harry Butler Institute, Murdoch University, Murdoch, WA 6150, Australia

Correspondence to: Giovanni Di Virgilio (giovanni.divirgilio@environment.nsw.gov.au; giovanni@unsw.edu.au)

1 **Abstract.** NARClIM 2.0 comprises two Weather Research and Forecasting (WRF) regional climate
2 models (RCMs) downscaling five CMIP6 global climate models contributing to the Coordinated
3 Regional Downscaling Experiment over Australasia at 20 km resolution, and south-east Australia at 4
4 km convection-permitting resolution. We first describe NARClIM 2.0's design, including selecting
5 two, definitive RCMs via testing seventy-eight RCMs using different parameterisations for planetary
6 boundary layer, microphysics, cumulus, radiation, and land surface model (LSM). We then assess
7 NARClIM 2.0's skill in simulating the historical climate versus CMIP3-forced NARClIM 1.0 and
8 CMIP5-forced NARClIM 1.5 RCMs and compare differences in future climate projections. RCMs
9 using the new Noah-MP LSM in WRF with default settings confer substantial improvements in
10 simulating temperature variables versus RCMs using Noah-Unified. Noah-MP confers smaller
11 improvements in simulating precipitation, except for large improvements over Australia's southeast
12 coast. Activating Noah-MP's dynamic vegetation cover and/or runoff options primarily improve
13 simulation of minimum temperature. NARClIM 2.0 confers large reductions in maximum temperature
14 bias versus NARClIM 1.0 and 1.5 (1.x), with small absolute biases of ~0.5K over many regions
15 versus over ~2K for NARClIM1.x. NARClIM 2.0 reduces wet biases versus NARClIM1.x by as much
16 as 50%, but retains dry biases over Australia's north. NARClIM 2.0 is biased warmer for minimum
17 temperature versus NARClIM 1.5 which is partly inherited from stronger warm biases in CMIP6

18 versus CMIP5 GCMs. Under shared socioeconomic pathway (SSP)3-7.0, NARClIM 2.0 projects ~3K
19 warming by 2060-79 over inland regions versus ~2.5K over coastal regions. NARClIM 2.0-SSP3-7.0
20 projects dry futures over most of Australia, except for wet futures over Australia's north and parts of
21 western Australia which are largest in summer. NARClIM 2.0-SSP1-2.6 projects dry changes over
22 Australia with only few exceptions. NARClIM 2.0 is a valuable resource for assessing climate change
23 impacts on societies and natural systems and informing resilience planning by reducing model biases
24 versus earlier NARClIM generations and providing more up-to-date future climate projections
25 utilising CMIP6.

Keywords:

26 Climate change; climate impact adaptation; dynamical downscaling; CORDEX-CMIP6; model
27 design; model evaluation

28 **1. Introduction**

29 Climate projections are foundational to informing climate change mitigation and adaptation planning
30 at various spatial scales (IPCC, 2021). Regional climate models (RCMs) dynamically downscale
31 global climate models (GCMs) at ~100-200 km resolution to simulate higher resolution climate
32 projections that better resolve local-scale influences on regional climate, such as mountain ranges,
33 land-use variation, land-sea contrasts, and convective processes (Torma et al., 2015; Giorgi, 2019). As
34 such, whilst GCMs are the best tools for investigating climate at global scales, RCMs provide
35 improved guidance for climate policy at regional scale, which is the scale at which climate change
36 impacts are experienced (Hsiang et al., 2017).

37 The NARcliM programme (New South Wales and Australian Regional Climate Modelling) is
38 now in its third generation. Like its predecessors, NARcliM version 2.0 ('NARcliM 2.0'), aims to
39 produce robust, detailed regional climate projections at spatial scales relevant for use in local-scale
40 climate change analysis. A key feature of all NARcliM generations is to simulate the climate over the
41 Coordinated Regional Downscaling Experiment (CORDEX)-Australasia domain, and a higher
42 resolution inner domain over southeast Australia via one-way nesting (Figure 1). With one-way
43 nesting the inner domain obtains its initial and lateral boundary conditions from the simulation over
44 CORDEX-Australasia. NARcliM 1.0 simulated the climate of Australasia for three periods (1990-
45 2009, 2020-2039, 2060-2079) at 50 km resolution and southeast Australia at 10 km using three
46 configurations of the weather research and forecasting (WRF) RCM (Skamarock et al., 2008) to
47 downscale GCMs from Coupled Model Intercomparison Project phase three (CMIP3) under the SRES
48 A2 greenhouse gas (GHG) scenario (Evans et al., 2014). NARcliM 1.5 used CMIP5 GCMs under
49 representative concentration pathways (RCP) 4.5 and 8.5 to simulate continuously for 1950-2100 on
50 the same grids as NARcliM 1.0 using two of its RCMs (Nishant et al., 2021).

51 NARcliM 2.0 aims to improve performance in simulating the Australian climate relative to
52 previous NARcliM generations with the goal of better informing community resilience to climate
53 change (New South Wales Government, 2022, 2023). All NARcliM projects include a bottom-up
54 design ethos involving multi-sectoral end-user engagement in specifying model requirements to
55 ensure model performance and outputs meet end-user needs. Key requirements from the NARcliM
56 2.0 user-consultation include providing increased detail in climate simulations via higher resolution
57 and improving the simulation of precipitation and temperature as these are fundamental inputs to
58 climate impact studies. Whilst NARcliM 1.0 and 1.5 (1.x) confer the expected level of performance
59 in simulating the Australian climate (Di Virgilio et al., 2019; Evans et al., 2020b), recent
60 technological and scientific advancements mean that aspects of their performance might now be
61 improved. NARcliM1.x RCMs show widespread cold biases in maximum temperature exceeding
62 -5K for some RCMs. Conversely, minimum temperature is simulated more accurately with biases in

63 the range of $\pm 1.5\text{K}$. NARClIM1.x RCMs overestimate precipitation, particularly over Australia's
64 socio-economically important eastern seaboard (Di Virgilio et al., 2019).

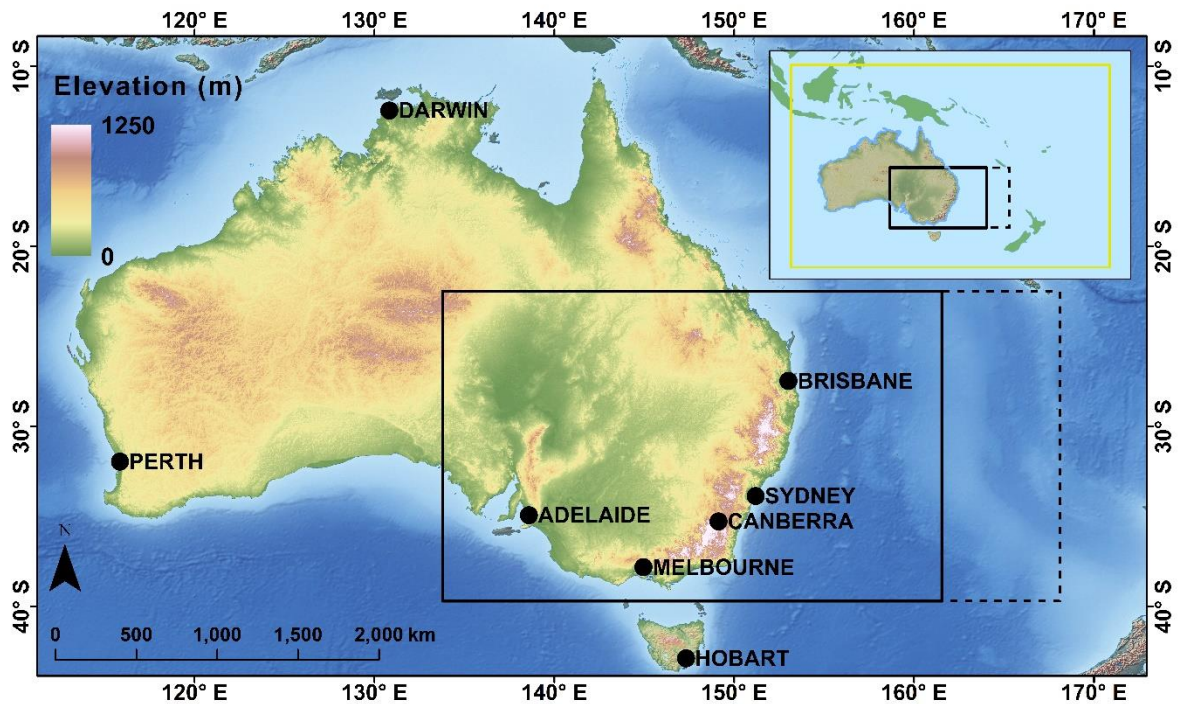
65 As they are expensive to run from both computational and data storage perspectives, dynamical
66 downscaling projects like NARClIM 2.0 use a subset of available GCMs as driving data, necessitating
67 careful model selection. Similarly, a large combination of different physical parametrisations
68 available for the WRF RCM enables many structurally different RCMs to be potentially used to
69 downscale GCMs. A key component of NARClIM 2.0's design is testing the viability of alternative
70 RCM parameterisations via a three-phase approach, with each phase building on the preceding phase
71 to identify the RCM parameterisations that perform well during testing to meet NARClIM 2.0's aim
72 of improving the simulation of Australia's climate. GCM and RCM statistical independence are also
73 sought to avoid creating a biased sample of climate change. Hence, the aims of this paper are to:

74 1) describe how and why NARClIM 2.0 differs from its predecessors in terms of its design and
75 production processes, explaining the model test and evaluation approaches underlying its design
76 decisions. A key focus is on the design and testing of seventy-eight structurally different WRF RCMs
77 and their evaluation to identify a subset of RCMs for use in NARClIM 2.0;

78 2) characterise the performance improvements of CMIP6-NARClIM 2.0 RCMs in simulating the
79 Australian climate relative to previous NARClIM generations by evaluating their skill in simulating
80 mean maximum and minimum temperature and precipitation versus observations;

81 3) summarise the climate projections produced by CMIP6-NARClIM 2.0 and how these differ
82 from previous CMIP3-5-NARClIM generations.

83 The following section summarises the basic design features of each NARClIM generation;
84 Section 3. describes evaluation methods and metrics; Section 4. describes NARClIM 2.0's design
85 process with a focus on its RCM physics testing, as well as a brief overview of its production process;
86 Section 5. summarises the RCM physics test results; Section 6. evaluates the performance of all
87 NARClIM models in simulating the recent Australian climate; Section 7. provides an overview of
88 their future projections; and Section 8. discusses key results and summarises this paper.



89

90 **Figure 1.** Model domains for NARClM regional climate simulations. The southeast inner domain for
 91 NARClM 2.0 is delineated with a solid black rectangle; the corresponding inner domain for NARClM 1.0 and
 92 1.5 is delineated with a dashed black line. The elevated terrain of the Australian Alps which form part of the
 93 Great Dividing Range is in eastern Australia. Inset shows the CORDEX-Australasia outer domain.

94 **2. Three generations of NARClM: model overviews**

95 The design of NARClM 1.0 is described in Evans et al. (2014); NARClM 1.5 used the same design
 96 approach but used CMIP5 rather than CMIP3 GCMs. All generations of NARClM use different
 97 versions of the WRF model to perform dynamical downscaling of GCMs since the WRF model goes
 98 through regular updates. The southeast Australian inner domain captures five of Australia's eight
 99 capital cities (Figure 1) and over 75% of the Australian population (Australian Bureau Statistics,
 100 2024). Additionally, the inner domain captures coastal regions that are characterised by topographic
 101 complexity and land-use class variation. Regions east of the Great Dividing Range mountains in
 102 southeast Australia (Figure 1) show different responses to oceanic climate modes compared to inland
 103 semi-arid regions (Murphy and Timbal, 2008) and are impacted by events such as rapidly developing
 104 storms, including east coast lows (Pepler and Dowdy, 2021). Such atmospheric processes are not
 105 adequately resolved by GCMs due to coarse resolutions (Di Virgilio et al., 2022; Grose et al., 2020).

106 NARClM 2.0 encompasses several design advancements over its predecessors (Table 1).
 107 NARClM 2.0 RCMs have a 20 km resolution CORDEX-Australasia domain (versus 50 km) and 4
 108 km (versus 10 km) domain over southeast Australia and use 45 (versus 30) vertical levels. The aim of
 109 increasing the resolution of this inner domain from 10 km to 4 km is to render these simulations

110 convection-permitting (Kendon et al., 2021; Lucas-Picher et al., 2021). Hence, whilst the 20 km-
111 resolution outer domain uses cumulus parametrisation, simulations over the 4 km domain do not use
112 cumulus parametrisation. NARClIM 2.0 also includes a new collaboration with the Western
113 Australian government, with separate 4 km simulations being performed over south-west and north-
114 west Western Australia (not shown in Figure 1) as part of the Western Australian climate science
115 initiative (DWER, 2023). Boundary conditions derived from the 20 km NARClIM 2.0 CORDEX
116 Australasia domain are used to drive these simulations. Additional major differences in model setup
117 for NARClIM 2.0 include:

- 118 ▪ NARClIM 1.0 RCMs use different parameterisations for planetary boundary layer (PBL)
119 physics, surface physics, cumulus physics, land surface model (LSM), and radiation (Evans et
120 al., 2014). These RCM parameterisations were also used for NARClIM 1.5. Owing to the pro-
121 ject aims stated above, RCM parameterisations for NARClIM 2.0 differ to those of NAR-
122 ClIM1.x (see Sect. 4).
- 123 ▪ NARClIM 2.0 increases the number of driving GCMs to 5 and simulates for a wider range of
124 plausible future climates via three shared socioeconomic pathways (SSP). SSP1-2.6 is select-
125 ed as a low GHG scenario envisaging a future climate with CO₂ emissions cut to net zero by
126 around 2075 and warming held to below 2°C by 2100; SSP2-4.5 estimates projected warming
127 under a ‘middle of the road’ scenario where temperatures increase to ~2.7°C by 2100; and
128 SSP3-7.0 is a high GHG scenario which assumes warming of ~4°C by 2100 (IPCC, 2021).
- 129 ▪ Urban physics is activated in NARClIM 2.0 (WRF setting: sf_urban_physics=1) to represent
130 surface energy balance in urban areas via a single layer urban canopy model (Kusaka and
131 Kimura, 2004).
- 132 ▪ Input of different aerosol species is activated for the RCM radiation scheme using the Tegen
133 et al. (1997) climatology available in WRF (aer_opt=1). This aerosol forcing is the same for
134 all GCMs, and not model-specific.
- 135 ▪ The eastern boundary of the NARClIM 2.0 inner domain is located further westward relative
136 to that of NARClIM1.x (Figure 1).

137 **Table 1.** High-level design features of three generations of NARCLiM regional climate models

| | Model Generation | | |
|--|------------------------------------|--------------------------------------|------------------------------------|
| | NARCLiM 1.0 | NARCLiM 1.5 | NARCLiM 2.0 |
| Release date | 2014 | 2020 | 2023-2024 |
| Years simulated | 1990-2009, 2020-2039, 2060-2079 | 1950-2100 | 1950-2100 |
| Grid resolutions: CORDEX-Australasia; NARCLiM inner domains | 50 km; 10 km | 50 km; 10 km | 20 km; 4 km |
| Vertical levels | 30 | 30 | 45 |
| Global Climate Models | 4 CMIP3 GCMs | 3 CMIP5 GCMs | 5 CMIP6 GCMs |
| Regional Climate Models | 3 RCM configurations (WRF3.3) | 2 RCM configurations (WRF3.6.0.5) | 2 RCM configurations (WRF4.1.2) |
| Future emission scenarios | SRES A2 | RCP4.5, RCP8.5 | SSP1-2.6, SSP2-4.5, SSP3-7.0 |
| Reanalysis-driven (CORDEX Evaluation) | NCEP: 1950-2009 | ERA-Interim: 1979-2013 | ERA5: 1979-2020 |
| Computational resources (core hours) | 30M | 30M | 1060M |

138 **3. Evaluation methods**

139 This section largely focuses on the methods and metrics used for the NARCLiM 2.0 RCM physics test-
140 ing and comparisons of model biases and future climate projections against previous generations of
141 NARCLiM. Details on methods and results for the CMIP6 GCM evaluation used to select driving
142 GCMs and the ERA5-NARCLiM 2.0 RCM evaluation used to select two, definitive RCMs for the
143 GCM-driven simulations are available in Di Virgilio et al. (2022) and Di Virgilio et al. (in review),
144 respectively, with overviews of these components of NARCLiM 2.0 design provided in Sections 4.2
145 and 4.4 below.

146 **3.1 Observations**

147 Australian Gridded Climate Data (AGCD version 1.0; Evans et al., 2020a) are the observational data
148 used to evaluate the NARClIM 2.0 RCM physics test RCMs. These daily gridded data for maximum
149 and minimum temperature and precipitation are obtained from an interpolation of station observations
150 across Australia. AGCD data are on a regular WGS84 grid with a grid-averaged resolution of 0.05°.
151 For the NARClIM 2.0 RCM physics tests, the AGCD data were re-gridded to correspond with the
152 RCM data from the inner domain on their native grids using a conservative area-weighted re-gridding
153 scheme. All data (RCM and AGCD) were restricted to a common extent contained within the inner
154 domain over southeast Australia, and a land mask was applied so that statistics were computed using
155 only land pixels. Treatment of AGCD for the CMIP6 GCM evaluation and the ERA5-NARClIM 2.0
156 RCM evaluation is described in Di Virgilio et al. (2022) and Di Virgilio et al. (in review), respective-
157 ly.

158 **3.2 Methods and metrics: phase I-III NARClIM2.0 physics tests**

159 Test RCM performances in reproducing observations for daily maximum and minimum temperature
160 and daily precipitation were assessed by calculating the model bias, i.e., model outputs minus AGCD,
161 and the RMSE of modelled versus observed fields. Model biases and RMSEs were calculated at an-
162 nual and seasonal timescales. The model representations of the hottest and the wettest day on an an-
163 nual time scale over the study region were also compared with AGCD. Probability density functions
164 (PDFs) were calculated for each variable using daily data. The Perkins skill score (PSS) (Perkins et
165 al., 2007) was calculated to assess the overall degree of overlap between modelled and observed dis-
166 tributions, with PSS = 1 indicating that distributions overlap perfectly.

167 There are several methods to evaluate the overall performance of RCMs. In this study, we
168 ranked the RCMs individually based on their bias, RMSE, and PSS for maximum temperature, mini-
169 mum temperature, and precipitation. Each variable was ranked separately for each metric. The ranks
170 were then summed to determine the overall ranking for each RCM.

171 **3.3 Independence assessments**

172 We used the method of Bishop and Abramowitz (2013) as one of two methods of assessing the inde-
173 pendence of physics test RCMs and the target CMIP6 GCMs under evaluation for use in NARClIM
174 2.0. This approach uses the covariance in model errors as the basis to define model dependence; spe-
175 cifically, independence coefficients are derived from the error covariance matrix of the RCMs or
176 GCMs. Model independence is quantified using the correlation of model errors. For the physics test
177 RCMs, errors are computed by comparing the climatology of maximum and minimum temperature
178 and precipitation over the south-east Australia inner domain for 2016 with corresponding AGCD ob-

179 servations. The same calculation is performed for the CMIP6 GCMs, except for the Australian conti-
180 nent. Daily timeseries of precipitation, maximum and minimum temperature are calculated individual-
181 ly for each RCM and for AGCD. The simulated and observed daily timeseries of each variable are
182 then normalised by the standard deviation of the corresponding observed variable. These normalised
183 variables are concatenated for each RCM (GCM) and AGCD. An anomaly time series for each grid
184 cell is then produced. These time series are used to create a model error covariance matrix containing
185 the errors for all RCMs (GCMs). The coefficients of a linear combination of the RCMs (GCMs) that
186 optimally minimises the mean square error depends on both model performance and model depend-
187 ence (Bishop and Abramowitz, 2013). The result of this minimisation problem is written in terms of
188 the covariance matrix. The magnitude of coefficients assigned to each RCM (GCM) reflects a combi-
189 nation of their performance and independence. Highly independent models have different errors when
190 simulating the recent climate. Models with the largest coefficients have the most independent errors
191 versus observations.

192 The Herger method of subset selection (Herger et al., 2018), as implemented here, uses quad-
193 ratic integer programming to find the subset of models whose equally-weighted subset mean (EWSM)
194 minimises a quadratic cost function. This cost function is chosen to measure the performance of the
195 EWSM in comparison to a given observational product. The two cost functions used here are: the
196 mean squared error (MSE) between the EWSM and the observational product (Herger et al. 2018, Eq.
197 1); and another which measures a combination of the MSE of the EWSM, the average MSE of each
198 subset member, and the average pairwise mean squared distance between subset members (Herger et
199 al. 2018, Eq. 2).

200 **3.4 NARcliM2 CMIP6-RCMs: historical evaluation and climate change** 201 **projections**

202 Performances of NARcliM 2.0 versus NARcliM1.x RCMs in reproducing the recent Australian cli-
203 mate are evaluated by calculating the model biases (model outputs minus AGCD observations) for
204 mean maximum and minimum temperature and precipitation for 1990-2009. To enable comparison of
205 future projections between NARcliM 1.0, NARcliM 1.5 and NARcliM 2.0 (where NARcliM 1.0
206 modelled for 1990-2009, 2020-2039, and 2060-2079), all NARcliM ensemble projected changes are
207 shown as far future (2060–2079) minus present day (1990–2009).

208 **3.5 Statistical significance**

209 When quantifying RCMs' future climate change projections (compared to the historical period) and
210 biases in maximum and minimum temperature, the statistical significance is calculated for each grid
211 cell using t-tests assuming equal variance. The Mann–Whitney U test is used for precipitation given
212 its non-normality. Significance thresholds were adjusted to account for multiple testing using Walk-

er's test (Eq.2 in Wilks, 2016). For individual RCMs, grid cells showing statistically significant changes are stippled, otherwise they are shown in colour where change is statistically insignificant. Results on the statistical significance of each ensemble mean are separated into three categories following Tebaldi et al. (2011): 1) statistically insignificant areas are shown in colour, denoting that less than 50% of RCMs are significantly biased/different; 2) in areas of significant agreement (stippled), at least 50% of RCMs are significantly biased/different and at least 70% of significant models in the CMIP6-NARClIM 2.0 RCM ensemble agree on the sign of the bias/difference. In such areas, many ensemble members have the same bias sign which is an undesirable outcome; and 3) areas of significant disagreement, where at least 50% of RCMs are significantly biased/different and fewer than 70% of significant models agree on the bias sign, are shown with diagonal hatching for the CMIP6-NARClIM 2.0 historical evaluation and climate change signals.

4. NARClIM 2.0 design and production process overview

The NARClIM 2.0 design and production processes are summarised below in reference to Figure 2. The design process is an adaptation of that introduced in Evans et al. (2014). Two companion manuscripts describe elements shown in Figure 2, which are therefore only summarised briefly in this manuscript: Di Virgilio et al. (2022) describes the CMIP6 GCM selection process summarised in Box 2, and Di Virgilio et al. (in review) describes the ERA5-RCM evaluation undertaken in Boxes 5 and 6.

I. Design Phase:

- i) **Box 1:** model design requirements are identified via consultation between NARClIM 2.0 modelling groups and multi-sectoral end-users, as well as adherence to CORDEX-CMIP6 design requirements (WCRP, 2020).
- ii) **Box 2:** NARClIM1.x selected driving CMIP3-5 GCMs (respectively) via literature review of existing GCM evaluations. During NARClIM 2.0 design, there were no pre-existing comprehensive evaluations of individual CMIP6 GCMs for the Australian region, including assessments of climate change signals and GCM statistical independence. Hence, an evaluation and selection of CMIP6 GCMs was conducted (see Di Virgilio et al. 2022). This evaluation selected five GCMs to force two NARClIM 2.0 RCMs (see Sect 4.2 and 4.4). The relative contribution to uncertainty/variation in climate projections can be larger for GCMs than for RCMs (e.g. Lee et al., 2023).
- iii) **Boxes 3-4:** a new WRF RCM multi-physics test ensemble is created for NARClIM 2.0: RCM physics testing is conducted via a three-phase approach, with each phase building on the findings of the preceding phase to identify the RCM parameterisations that perform well during testing with the aim of improving the simulation of the Australian climate. In this way, RCMs are parameterised with different physics settings via each test phase, sys-

248 tematically removing poor performing options while facilitating the fine tuning and im-
249 provement of the parameterisations that perform well during testing to build a total en-
250 semble size of seventy-eight structurally different test RCMs. The performance of the dif-
251 ferent test RCM configurations is evaluated, ultimately leading to the selection of a subset
252 of seven RCMs for subsequent downscaling of ERA5 reanalysis as part of the CORDEX
253 evaluation experiment.

254 iv) **Boxes 5-6:** These seven RCMs are used to downscale ERA5 reanalysis over the 20 km
255 and 4 km domains for 1979-2020. Evaluating these ERA5-forced simulations informs se-
256 lection of two definitive, production RCMs for CMIP6-forced downscaling (see Sect. 4.4
257 and Di Virgilio et al. in review).

258 II. Production Phase:

259 i) **Boxes 7-8:** CMIP6 GCM data are pre-processed to create initial and boundary conditions
260 to drive simulations for the historical (1950-2014) and SSP experiments (2015-2100). A
261 code repository used for this GCM preprocessing is available on Zenodo at:

262 <https://doi.org/10.5281/zenodo.11184830> within the WRF/repo_snapshots subdirectory.

263 Quality assurance/quality control (QA/QC) is performed on these data before initiating
264 the simulations (e.g. variables are checked to confirm data do not contain significant out-
265 liers across ensemble members).

266 ii) **Boxes 9-11:** the 151-year CMIP6-forced NARCLiM 2.0 RCM simulations are run using
267 National Computational Infrastructure at Canberra, Australia (NCI, <https://nci.org.au/>).
268 File integrity verification and QA/QC are performed on each year of raw WRF output
269 throughout the simulation lifecycle and prior to post-processing to CORDEX-compliant
270 format climate variables. QA/QC tests include calculating the minimum, maximum, mean
271 and standard deviation for key variables over consecutive periods of six simulation days.
272 Variables are categorised as either normally distributed or otherwise. Normally distribut-
273 ed variables (e.g. surface temperature) are deemed potentially erroneous if their mini-
274 ma/maxima are greater than five standard deviations away from the global mean of the
275 relevant statistic of the rolling six-day period. Non-normally distributed variables (e.g.,
276 snow depth and precipitation) are checked only for global minima and maxima.

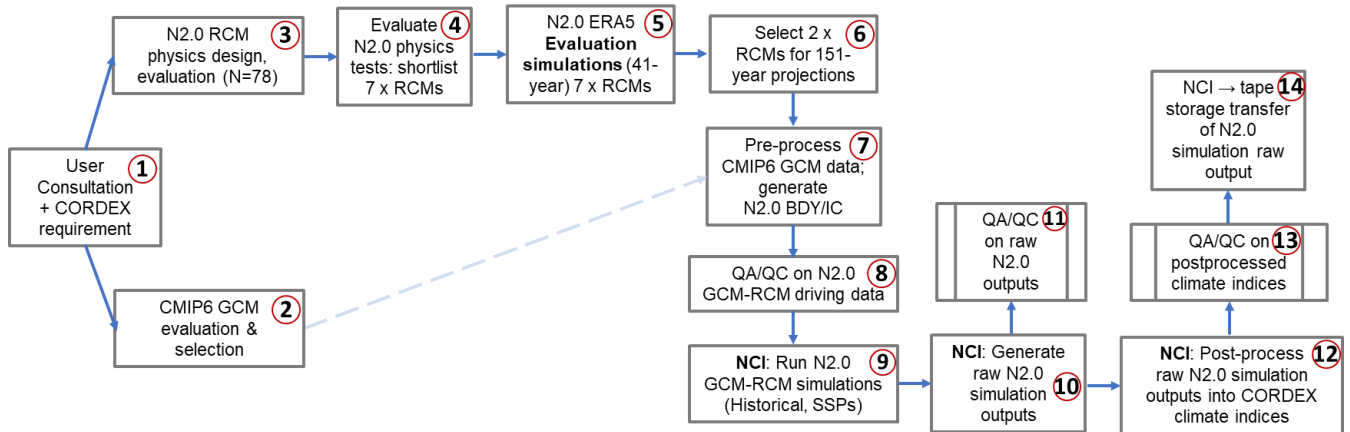
277 iii) **Boxes 12-13:** after each year of simulation raw output is generated, their post-processing
278 is initiated to produce CORDEX CORE, Tier 1 and Tier 2 variables (WCRP, 2022). A
279 statistical QA/QC process is automatically applied to each year of post-processed
280 CORDEX CORE variables as they are generated throughout the simulations. QA/QC
281 tests include:

- 282 ▪ Check for presence of missing values.
- 283 ▪ Check that all values are within realistic ranges for minima and maxima.

- 284 ▪ Check minima and maxima are not equal at any timestep with exceptions (e.g.,
- 285 snow depth which can be zero everywhere in the outer domain).
- 286 ▪ Check that changes over time are within realistic ranges (i.e., assess temporal
- 287 gradients).
- 288 ▪ Check that changes between neighbouring data points are within realistic ranges
- 289 (i.e., assess spatial gradients).
- 290 ▪ Check the number of grid cells with NaN (non-numerical) values do not exceed
- 291 the threshold set for the variable.

292 Reasonable ranges for variables are determined using a series of threshold values that are
 293 based on historical records and/or empirical analysis. QA/QC computer scripts generate
 294 exceedance files which output every data point that surpasses the threshold values, and
 295 these exceedance files are then manually reviewed to determine whether an issue is a true
 296 or false positive, etc.

297 iv) **Box 14:** Once each year of WRF raw files is post-processed, raw files are transferred to a
 298 tape facility for long-term storage.



299
 300 **Figure 2.** Simplified overview of NARCIIM 2.0 (N2.0) design and production processes. ERA5 = ECMWF
 301 Reanalysis v5 data; BDY = boundary conditions; IC = Initial conditions; QA/QC = Quality Assurance / Quality
 302 Control; NCI = National Computational Infrastructures (high performance computer used to run N2.0
 303 simulations).

304 These model design and production stages are now described in more detail:

305 4.1 Model evaluation and selection

306 Practical constraints such as available compute and data storage resources enforce an upper limit on
 307 GCM-RCM ensemble size. Thus, NARCIIM 2.0 uses a subset of available CMIP6 GCMs and WRF
 308 RCM configurations, necessitating careful GCM and RCM selection to create a subset of GCM-

309 RCMs that provide robust climate simulations whilst also adequately sampling model uncertainty. In
310 selecting a subset of GCMs and RCMs for dynamical downscaling, it is desirable to reject models that
311 perform consistently poorly relative to their peers in simulating the current climate, as this provides
312 lower confidence in the projected change (Evans et al., 2020b; Di Virgilio et al., 2022; Grose et al.,
313 2023). Furthermore, the modelled climate space sampled is reduced when selecting a subset of GCMs,
314 which can create a biased view of the climate, as well as the plausible change in climate. Care must
315 therefore be taken to ensure that the subset of models used for downscaling are representative of the
316 full range of possible climates, and that model errors are uncorrelated, i.e., that models are statistically
317 independent. The steps taken to evaluate and select GCMs and RCMs for NARClIM 2.0 are described
318 next.

319 **4.2 CMIP6 GCM evaluation**

320 A three-phase process was used to evaluate individual CMIP6 GCMs (for further details see Di
321 Virgilio et al. 2022):

322 **4.2.1 CMIP6 GCM Performance**

323 We evaluated the performances of individual CMIP6 GCMs in simulating the following aspects of the
324 observed historical climate of Australia:

- 325 ▪ annual and seasonal climatologies and daily distributions of maximum and minimum temper-
326 atures and precipitation.
- 327 ▪ climate extremes, such as the 99th percentiles of daily maximum temperature and precipita-
328 tion, and the 1st percentile of minimum temperature.
- 329 ▪ teleconnections of oceanic climate modes and Australian regional rainfall.

330 Temperature and precipitation variables are chosen for evaluation because, being well-represented in
331 high-quality gridded observational data sets for the Australian continent, they provide the most direct
332 comparison to observations (King et al., 2013). They are also often prioritised for impact studies.
333 Given variables such as winds (U, V), air temperature (T), water mixing ratio (Q), geopotential height
334 (Z), sea surface temperature (SST), and sea level pressure (PSL) serve as boundary conditions for
335 driving RCMs, these could be incorporated into future GCM evaluation studies. However, evaluating
336 such variables would require use of re-analysis data as surrogate observations.

337 A set of GCMs that performed consistently poorly across the variables and statistics
338 considered were identified. These models, as well as those with insufficient data to enable dynamical
339 downscaling using the WRF RCM, were excluded from further evaluation leaving 27 GCMs for
340 subsequent assessment.

341 **4.2.2 CMIP6 GCM Independence**

342 The retained 27 GCMs were subjected to the Bishop and Abramowitz (2013) and Herger et al. (2018)
343 independence analyses (see Sect. 3.5). The GCMs were then ranked according to their relative level of
344 statistical independence.

345 **4.2.3 Sampling CMIP6 GCM Climate Change Spread**

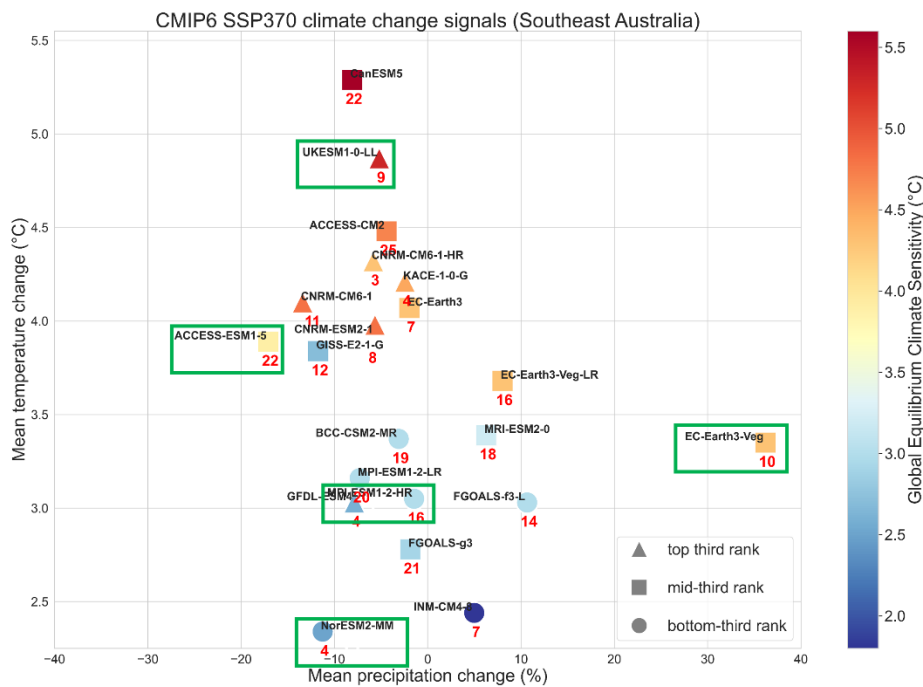
346 For climate change risk assessments, climate projections should reflect as much of the range of
347 plausible future climate changes as possible (Whetton and Hennessy, 2010). The subset of CMIP6
348 GCMs selected for NARClIM 2.0 spanned a wide range of future changes in annual mean temperature
349 and precipitation. Climate change signals were calculated for 2080-2099 minus 1995-2014 for the
350 Australian continent and south-east Australia under SSP3-7.0 (for the latter, see Figure 3). The GCM
351 independence rankings were placed within this climate change space, with higher independence
352 rankings viewed as favourable, along with consideration of the following criteria:

- 353 i) A balanced range of GCM Equilibrium Climate Sensitivities (ECS) were sampled. ECS is the
354 long-term increase in global mean surface air temperature in response to the radiative forcing
355 caused by a doubling of pre-industrial CO₂ concentrations. ECS is related to global tempera-
356 ture change, not just changes over Australia, however, it correlates strongly with regional
357 warming. Around one third of CMIP6 GCMs show ECS values higher than the upper end of
358 the likely range of 2.5°C to 4°C (IPCC, 2021). An upper range of > ~5°C cannot be ruled out
359 (Meehl et al., 2020; Bjordal et al., 2020; Sherwood et al., 2020).
- 360 ii) Some CMIP6 GCMs that are favourable in terms of model performance and independence
361 could not be selected as input to WRF for NARClIM 2.0 owing to insufficient data availabil-
362 ity for key variables, where ideally, WRF requires sub-daily data for the variables shown in
363 Supporting Information, Table S1.

364 As a result of the above process, the five CMIP6 GCMs listed in Table 2 are selected to force each of
365 the two definitive NARClIM 2.0 RCMs selected via the RCM physics testing and ERA5 evaluation
366 processes.

367 **Table 2.** Basic details of the CMIP6 GCMs used to force the two definitive RCMs comprising the
368 NARClIM 2.0 CORDEX-CMIP6 ensemble.

| CMIP6 GCM | Institution | Variant/Run | Atmosphere lat/lon grid (°) |
|---------------|--|-------------|-----------------------------|
| ACCESS-ESM1-5 | CSIRO | r6i1p1f1 | 1.2 × 1.8 |
| EC-Earth3-Veg | EC-EARTH consortium | r1i1p1f1 | 0.7 × 0.7 |
| MPI-ESM1-2-HR | Max Planck Institute for Meteorology (MPI) | r1i1p1f1 | ~0.9 |
| NorESM2-MM | Norwegian Climate Centre | r1i1p1f1 | 0.9 × 0.9 |
| UKESM1-0-LL | UK Met Office and NERC research centres | r1i1p1f2 | 1.3 × 1.9 |



369
 370 **Figure 3.** CMIP6 GCM climate change signals (2080-2099 versus 1995-2014) over south-east Australia for the
 371 subset of GCMs retained following the model performance evaluation in Di Virgilio et al. (2022), and that
 372 simulated at least monthly mean near surface air temperature and precipitation for the SSP-3.70 scenario. Boxed
 373 GCMs are selected to force NARcliM 2.0 RCMs. Marker shapes indicate overall GCM performance; markers
 374 are coloured according to their global equilibrium climate sensitivity (ECS) values; **Red** numbers represent the
 375 smallest Herger Method 1 set for that GCM.

376 4.3 NARcliM 2.0 RCM physics testing

377 The NARcliM 2.0 RCM physics testing aims to identify and exclude RCMs that perform consistently
 378 poorly in simulating the southeast Australian climate and to select RCMs that have high statistical
 379 independence. The selection of RCMs in NARcliM 2.0 involves the creation of a multi-physics
 380 ensemble where each RCM uses different physical parametrisations for PBL, microphysics, cumulus,
 381 radiation, and LSM. This enables many structurally different RCMs to be constructed and tested. In
 382 NARcliM 1.0, 36 WRF RCM configurations were designed, tested, and evaluated (Evans et al.
 383 2014). NARcliM 2.0 physics testing assesses 78 RCM configurations which are progressively tested
 384 via three phases, where each test phase is informed by the outcomes of the preceding phase to
 385 systematically remove poor performing RCM options while facilitating the selection of
 386 parameterisations that perform well during testing. The N=36 RCMs tested for NARcliM 1.0 were
 387 evaluated based on eight representative storm event simulations each of two-weeks duration (Evans et
 388 al. 2014). NARcliM 2.0 physics simulations were run over an entire annual cycle (2016) with a two-
 389 month spin-up period commencing 1 November 2015. Australia experienced a range of weather
 390 extremes during 2016 driven by a range of climatic influences making 2016 a suitable target year
 391 (Bureau of Meteorology, 2017). Whilst assessing RCMs for an entire year improves on assessing for

392 discrete storm events as per physics testing for NARCLiM 1.0, it was not feasible to run a large RCM
 393 physics ensemble for a longer duration. Initial and boundary conditions for all phases of the
 394 NARCLiM 2.0 RCM physics test simulations were derived from the ERA-Interim reanalysis data set
 395 (Dee et al., 2011). ERA-Interim was used because ERA5 was not available at the time. The three
 396 phases of NARCLiM 2.0 physics testing are as follows:

397 **4.3.1 Phase I (N=36)**

398 Thirty-six RCMs were evaluated in Phase I. One radiation scheme (RRTMG) was tested for both long
 399 and short-wave radiation (it was held fixed for all RCMs), whereas physics settings for PBL,
 400 microphysics, cumulus, and LSM were varied. Of the 36 simulations, 18 used the Noah-Unified LSM,
 401 whilst the remainder used Community Land Model version 4.0 (CLM4). The physics options tested
 402 are listed in Table 3, where these were selected based on literature review. Each physics test
 403 simulation is denoted by a 12-digit identifier which comprises 6 pairs of digits, with each pair
 404 corresponding to the choice of a specific physics option as specified in the WRF namelist.input file.
 405 These pairs of digits follow the order: planetary boundary layer (pbl) | cloud microphysics (mp) |
 406 cumulus convection (cu) | shortwave radiation (sw) | longwave radiation (lw) | LSM (sf) and
 407 correspond to the WRF namelist options shown in Table 3. For example, the simulation
 408 050601040402 is interpreted as: 05 | 06 | 01 | 04 | 04 | 02 and denotes that this simulation uses the
 409 following physics settings:

bl_pbl_physics = 05 (MYNN2)
 mp_physics = 06 (WSM6)
 cu_physics = 01 (Kain-Fritsch)
 ra_sw_physics = 04 (RRTMG)
 ra_lw_physics = 04 (RRTMG)
 sf_surface_physics = 02 (Noah Unified)

410 The complete set of WRF RCM configurations tested in Phase I is shown in Supporting Information
 411 Table S2.

412 **Table 3.** Physics options used in phase I (N=36) tests.

| Physics Option Description | WRF Namelist | Options Tested | Reference |
|----------------------------|----------------|-------------------|--------------------------|
| Planetary boundary layer | bl_pbl_physics | 01 = YSU | Hong et al. (2006) |
| | | 05 = MYNN2 | Nakanishi & Niino (2009) |
| | | 07 = ACM2 | Pleim (2007) |
| Microphysics | mp_physics | 06 = WSM6 | Hong and Lim (2006) |
| | | 08 = Thompson | Thompson et al. (2008) |
| Cumulus parameterisation | cu_physics | 01 = Kain-Fritsch | Kain (2004) |
| | | 02 = BMJ | Janjić (2000) |
| | | 06 = Tiedtke | Tiedtke (1989) |

| | | | |
|---------------------|--------------------|------------------------------|----------------------|
| Shortwave radiation | ra_sw_physics | 04 = RRTMG | Iacono et al. (2008) |
| Longwave radiation | ra_lw_physics | 04 = RRTMG | |
| Land surface model | sf_surface_physics | 02 = Noah-Unified | Tewari et al. (2016) |
| | | 05 = Community Land Model V4 | Oleson et al. (2010) |

413 **4.3.2 Phase II (N=60): additional LSM and radiation scheme tests**

414 Phase I RCMs using CLM4.0 were omitted from further testing because they did not consistently im-
415 prove performance in simulating the Australian climate relative to RCMs using Noah-Unified. In ad-
416 dition, RCMs using CLM4.0 had increased simulation times (by approximately twice when compared
417 to Noah-Unified). Hence, Phase II focused exclusively on further testing of the RCM configurations
418 that used the Noah-Unified LSM.

419 The physics settings tested in Phase II are an alternative LSM to Noah-Unified (Noah Multi-
420 Parameterisation; Noah-MP, Niu et al., 2011) and New Goddard radiation (Chou et al., 2001). Owing
421 to time/resource constraints, testing all eighteen Phase I RCMs using Noah-Unified was not feasible.
422 To reduce the number of RCMs for further testing, the worst-performing Noah-Unified based RCM
423 configurations identified in Phase I were excluded. The N=18 RCMs using Noah-Unified are listed
424 along with their overall performance total scores in Table 4 where the lowest scores under Rank totals
425 indicate the RCMs that overall perform relatively well versus their peers (see Sect. 3 Evaluation
426 Methods). Note that the Overall rank denotes the RCMs' relative ranking among all Phase I RCMs.
427 There is a sharp reduction in rank totals for RCMs #13-18 inclusive, relative to RCMs #1-12. There-
428 fore, RCMs #13-18 are excluded from further testing, and RCMs #1-12 are retained.

429 **Table 4.** RCM physics combination ranks of the Phase I, N=18 Noah Unified (NU) based RCMs.

430 Scores/ranks are based on model bias and root mean square error for annual and seasonal precipita-
431 tion, minimum temperature, maximum temperature, climate extremes (wettest and hottest days), and
432 Perkins Skill Scores (see Sect. 3). RCMs #1-12 are selected for further testing.

| RCM # | RCM ID | Physics combination | | | | | Rank total | Overall rank in N=36 Phase I |
|-------|--------------|---------------------|----------|---------|-------|-----|------------|------------------------------|
| | | PBL | MP | Cumulus | SW/LW | LSM | | |
| 1 | 070801040402 | ACM2 | Thom | KF | RRTMG | NU | 484 | 1 |
| 2 | 070601040402 | ACM3 | WSM6 | KF | RRTMG | NU | 495 | 2 |
| 3 | 070802040402 | ACM4 | Thom | BMJ | RRTMG | NU | 527 | 3 |
| 4 | 070602040402 | ACM5 | WSM6 | BMJ | RRTMG | NU | 559 | 4 |
| 5 | 010802040402 | YSU | Thom | BMJ | RRTMG | NU | 574 | 7 |
| 6 | 050801040402 | MYNN2 | Thom | KF | RRTMG | NU | 583 | 8 |
| 7 | 010801040402 | YSU | Thompson | KF | RRTMG | NU | 617 | 11 |
| 8 | 050802040402 | MYNN2 | Thompson | BMJ | RRTMG | NU | 630 | 12 |

| | | | | | | | | |
|----|--------------|-------|----------|---------|-------|----|-----|----|
| 9 | 070606040402 | ACM2 | WSM6 | Tiedtke | RRTMG | NU | 639 | 13 |
| 10 | 050601040402 | MYNN2 | WSM6 | KF | RRTMG | NU | 662 | 16 |
| 11 | 070806040402 | ACM2 | Thompson | Tiedtke | RRTMG | NU | 662 | 16 |
| 12 | 010602040402 | YSU | WSM6 | BMJ | RRTMG | NU | 674 | 19 |
| 13 | 010601040402 | YSU | WSM6 | KF | RRTMG | NU | 702 | 23 |
| 14 | 010606040402 | YSU | WSM6 | Tiedtke | RRTMG | NU | 759 | 25 |
| 15 | 050606040402 | MYNN2 | WSM6 | Tiedtke | RRTMG | NU | 766 | 27 |
| 16 | 050602040402 | MYNN2 | WSM6 | BMJ | RRTMG | NU | 811 | 31 |
| 17 | 010806040402 | YSU | Thompson | Tiedtke | RRTMG | NU | 830 | 34 |
| 18 | 050806040402 | MYNN2 | Thompson | Tiedtke | RRTMG | NU | 857 | 35 |

433 This gives two sets of physics combinations for additional testing: 1) one replaces only RRTMG
434 (|04|04|) for short and longwave radiation with New Goddard (|05|05|) making no other changes; and
435 2) RRTMG radiation is retained, but Noah-MP (|04|) replaces Noah-Unified (|02|). This creates an
436 additional 24 RCM configurations for assessment, bringing the total RCMs tested to 60. Although
437 Noah-MP has several parameter options, Phase II uses its default settings.

438 **4.3.3 Phase III (N=78): parameterising Noah-MP**

439 Phase II shows that RCM performance using New Goddard radiation is generally inferior to the same
440 RCMs using RRTMG (see Sect. 5. RCM Physics test results). Consequently, RRTMG radiation is re-
441 adopted for Phase III. Conversely, a general performance improvement is conferred by using Noah-
442 MP over Noah-Unified (Sect. 5). Given this performance improvement using Noah-MP with default
443 settings, Phase III assesses RCM performances using specific parameter settings for Noah-MP.

444 Noah-MP provides a dynamic vegetation cover model option (referred to as dynamic vegeta-
445 tion in the WRF users' guide) (Niu et al., 2011). When deactivated (the default), monthly leaf area
446 index (LAI) is prescribed for various vegetation types and the greenness vegetation fraction (GVF)
447 comes from monthly GVF climatological values. Conversely, when dynamic vegetation cover is acti-
448 vated, LAI and GVF are calculated using a dynamic leaf model. We clarify here that dominant plant-
449 functional types do not change when using this option, but only the LAI and GVF, i.e., only the
450 amount of green cover changes.

451 Noah-MP also provides several options for modelling surface run-off and groundwater pro-
452 cesses including a TOPMODEL (TOPography based hydrological MODEL)-based surface runoff
453 scheme and a simple groundwater model (SIMGM; Niu et al., 2011). Some studies have shown that
454 using this option improves the modelling of soil moisture (e.g. Zhuo et al., 2019). Thus, three new sets
455 of physics configurations are tested using Noah-MP where default options for specific settings are
456 changed as follows:

- 457 4. activate dynamic vegetation cover (dveg=2 in the WRF namelist); no other changes.
- 458 5. activate TOPMODEL runoff with simple groundwater (opt_run=1); no other changes.

459 6. activate both dynamic vegetation and TOPMODEL runoff with simple groundwater; no other
 460 changes.

461 As above, the worst performing RCMs in Phase II are excluded from Phase III testing. Based
 462 on the RCM configuration performance rankings (Table 5), there is a sharp reduction in performance
 463 starting from RCM #7 inclusive. Therefore, RCMs #7-12 are excluded from further testing. Phase III
 464 thus comprises 18 new test simulations (sets 1-3 each comprising 6 RCMs) bringing the total RCMs
 465 tested to N=78. Phase III physics tests are denoted using the same RCM identification schemes distin-
 466 guished by appending set_1, set_2, set_3 to identifiers.

467 **Table 5.** RCM physics combination ranks of the Phase II Noah-MP RCMs. Scores/ranks are based on model
 468 bias and root mean square error for annual and seasonal precipitation, minimum temperature, maximum temper-
 469 ature, climate extremes (wettest and hottest days), and Perkins Skill Scores (see Sect. 3).

| No. | Physics combination | Rank total |
|-----|---------------------|------------|
| 1 | 50801040404 | 721 |
| 2 | 70806040404 | 822 |
| 3 | 50802040404 | 848 |
| 4 | 70802040404 | 872 |
| 5 | 70601040404 | 880 |
| 6 | 50601040404 | 891 |
| 7 | 10802040404 | 988 |
| 8 | 70602040404 | 1005 |
| 9 | 70606040404 | 1028 |
| 10 | 10801040404 | 1042 |
| 11 | 70801040404 | 1056 |
| 12 | 10602040404 | 1264 |

470 **4.3.4 Shortlisting Physics Test RCMs for ERA5-NARClM 2.0 evaluation simulations**

471 Considering the complete NARClM 2.0 N=78 physics test ensemble, to identify physics test RCMs
 472 that perform poorly overall, RCMs are eliminated if they are in the lowest 1/3 for RCM performance
 473 ranks for any of maximum temperature, minimum temperature, precipitation, or for the overall model
 474 performance rank across these variables (see Sect. 5. RCM Physics test results). Under this scheme,
 475 20 RCMs remain. The independence measures are then applied to the remaining 20 RCMs to choose a
 476 final subset of 7 RCMs for ERA5-forced evaluation simulations (see Sect. 4.4). The ensemble size
 477 limit of N=7 is determined by available compute resources. These 7 candidate RCMs are assessed for
 478 potential use in the CMIP6 GCM-forced downscaling phase of NARClM 2.0 (Sect. 4.4 and Di Vir-
 479 gilio et al. in review).

480 **4.4 CORDEX ERA5-NARClIM 2.0 evaluation simulations**

481 NARClIM1.x performed production climate simulations using a two-phase process. Its RCM physics
482 testing selected definitive production-grade RCMs which were then used to downscale both reanalysis
483 data and CMIP3/5 GCMs. In contrast, for NARClIM 2.0, as described above the N=78 RCM physics
484 testing culminates in shortlisting 7 production-candidate RCMs which are used to downscale the
485 ERA5 reanalysis for 42-years (1979-2020). This enables assessment of the performances of these 7
486 shortlisted RCMs over a climatological period rather than the single year (2016) of the physics test-
487 ing, which helps ascertain that performance differences between shortlisted RCMs are robust across a
488 multi-decadal timescale capturing climatologically diverse years. The aim is that two definitive pro-
489 duction-grade RCMs can be selected for CMIP6-forced downscaling from these ERA5-forced
490 CORDEX evaluation simulations. Thus, the seven ERA5-NARClIM 2.0 RCMs were driven by
491 ERA5.0 boundary conditions for January 1979 to December 2020 using the model and nested domain
492 setups described above for NARClIM 2.0. The skill of these RCMs in simulating the recent Australian
493 climate was assessed as follows (see Di Virgilio et al. in review): annual and seasonal means were
494 calculated for maximum and minimum temperature and precipitation using monthly means for tem-
495 perature variables, and the monthly sum for precipitation. Extremes of maximum temperature and
496 precipitation (99th percentiles) and extreme minimum temperature (1st percentile) were calculated us-
497 ing daily data. RCM performances in reproducing observations over these timescales were assessed
498 by calculating model outputs minus observations (i.e., model bias), and the RMSE of modelled versus
499 observed fields. RCM skill in simulating distributions of observed variables was assessed by compar-
500 ing the PDFs for daily mean observations versus those of the RCMs. The ultimate outcome of these
501 ERA5-forced simulations and their evaluation is the selection of two definitive RCM configurations,
502 R3 and R5, to run the CMIP6-forced phase of NARClIM 2.0, see Di Virgilio et al. (in review) for fur-
503 ther details on the evaluation methods and results. Supporting Information Figure S1 shows the WRF
504 namelist settings for the R3 and R5 RCMs (see also Sect. 9. Code Availability).

505 **4.5 CORDEX CMIP6-forced NARClIM 2.0 simulations**

506 The ideal CMIP6 GCM variables and their frequencies required to run the WRF RCM are listed in
507 Table S1. A minority of variables in Table S1 are not available at sub-daily frequencies for every tar-
508 get GCM. This necessitates assumptions/data proxies to be made. For instance, soil moisture and soil
509 temperature variables were unavailable for some selected GCMs; hence, surrogate data, such as sur-
510 face temperature, were used for initialisation (noting that soil data are only used by the RCM at ini-
511 tialisation). In these cases, we investigated how long it took for uncertainty in the initial conditions to
512 disappear from the WRF output by analysing the regionally averaged soil moisture time series. The
513 data were regionalised according to the four Australian Natural Resource Management (NRM) re-

514 gions / climate zones (Supporting Information Figure S2) which are broadly aligned with climatologi-
515 cal boundaries (Fiddes et al., 2021) and with the IPCC reference regions (Iturbide et al., 2020). Time
516 series plots (Figure S3) show that soil moisture equilibrates to be within a normal range following
517 initialisation, indicating that the 12-month spin-up year (1950) is sufficient to account for the assump-
518 tions made at model initialisation.

519 Boundary and initial conditions were prepared using selected GCM data to run the 151-year
520 GCM-driven simulations using WRF version 4.1.2. The GCM-driven simulations were run and com-
521 pleted using the pre-defined RCM settings for the two definitive RCM configurations using the WRF
522 namelists in Supporting Information Figure S1 (see also Sect. 9. Code Availability). A cold restart
523 was performed on the last Historical experiment year (2014), thus enabling the SSP1-2.6 and SSP3-
524 7.0 experiments to be run for 2015-2100 concurrently with the Historical experiment. Testing the time
525 duration required for soil moisture to equilibrate from the cold start showed that 1 year is sufficient.
526 The 2014 cold start year is eventually overwritten by Historical runs initiated in 1950.

527 **5. RCM Physics test results**

528 **5.1 Phase I RCM performance summary**

529 The spatial variation and magnitudes for Phase I RCM biases and RMSEs for annual mean maximum
530 and minimum temperature and precipitation are shown in Figures 4-5, respectively. Overall, RCMs
531 are biased cold for maximum temperature (mean absolute bias for the ensemble mean = 1.18 K), and
532 warm-biased for minimum temperature (mean absolute bias = 1.31 K; Figure 4a-b). Maximum tem-
533 perature RMSE magnitudes are large over the elevated terrain of the southeast coast and over western
534 regions (Figure 5a). The simulation of precipitation shows biases of varying sign, with wet biases that
535 are strongest over eastern coastal regions (Figure 4c). Precipitation RMSEs are particularly large
536 along the eastern coastline (>15 mm), and generally show an east-west gradient, i.e., progressively
537 decreasing further inland from the coast (Figure 5c).

538 **5.2 Comparing Phase II Physics Test RCM performances versus Phase I**

539 **5.2.1 Climate Means**

540 Overall, the RCM ensemble using New Goddard (NG) radiation has inferior performance to the corre-
541 sponding RCMs using RRTMG in terms of annual/seasonal mean maximum temperature biases,
542 RMSEs, and PSS (Table 7). In contrast, NG confers superior performance for annual/seasonal mean
543 minimum temperature for these statistics. RCMs using NG show reduced biases for annual mean and
544 spring-time precipitation, but larger errors for DJF and JJA (Table 7). RMSEs for annual and seasonal
545 precipitation are similarly variable.

546 **Table 7.** Climate means performance: phase II physics tests (i.e., N=12 set 1 changing only RRTMG to New
547 Goddard (NG) and N=12 set 2 changing only land surface model (LSM) from Noah-Unified to Noah-MP
548 (NMP) compared with the phase I physics test RCMs that were shortlisted for further testing (N=12).

| Variable | Timescale | Bias | | | RMSE | | | PSS | | |
|-----------------------|-----------|------------------------------|----------------------------------|----------------------------------|------------------------------|----------------------------------|----------------------------------|------------------------------|----------------------------------|----------------------------------|
| | | Phase I (N=12) ensemble mean | Phase II (NG rad.) ensemble mean | Phase II (NMP LSM) ensemble mean | Phase I (N=12) ensemble mean | Phase II (NG rad.) ensemble mean | Phase II (NMP LSM) ensemble mean | Phase I (N=12) ensemble mean | Phase II (NG rad.) ensemble mean | Phase II (NMP LSM) ensemble mean |
| Temp. Max. (K) | Annual | 0.87 | 1.27 | 0.58 | 3.56 | 3.73 | 3.50 | 0.950 | 0.936 | 0.955 |
| | DJF | 0.74 | 1.29 | 0.63 | 4.41 | 4.70 | 4.43 | | | |
| | MAM | 1.40 | 2.06 | 0.83 | 3.68 | 3.92 | 3.55 | - | - | - |
| | JJA | 0.62 | 0.81 | 0.52 | 2.64 | 2.66 | 2.65 | | | |
| | SON | 0.87 | 1.04 | 0.66 | 3.25 | 3.32 | 3.20 | | | |
| Temp. Min. (K) | Annual | 1.35 | 0.95 | 1.2 | 3.53 | 3.41 | 3.42 | 0.927 | 0.941 | 0.931 |
| | DJF | 1.50 | 1.08 | 0.87 | 3.86 | 3.82 | 3.66 | | | |
| | MAM | 1.21 | 0.84 | 0.92 | 3.55 | 3.45 | 3.50 | - | - | - |
| | JJA | 0.82 | 0.51 | 0.91 | 3.00 | 2.92 | 3.00 | | | |
| | SON | 1.88 | 1.47 | 1.92 | 3.63 | 3.40 | 3.58 | | | |
| Prec. (mm) | Annual | 0.25 | 0.24 | 0.25 | 7.21 | 7.32 | 6.78 | 0.943 | 0.950 | 0.946 |
| | DJF | 0.41 | 0.53 | 0.49 | 8.28 | 8.83 | 8.85 | | | |
| | MAM | 0.32 | 0.32 | 0.25 | 5.91 | 6.47 | 5.53 | - | - | - |
| | JJA | 0.37 | 0.53 | 0.44 | 7.63 | 7.34 | 7.65 | | | |
| | SON | 0.34 | 0.22 | 0.39 | 6.68 | 6.18 | 6.92 | | | |

549 Phase II RCMs using Noah-MP with RRTMG retained show improved performance in simu-
550 lating mean maximum and minimum temperature at annual timescales and most seasons relative to
551 corresponding Phase I RCMs using Noah-Unified (Table 7; Figure 4-5). For instance, the mean abso-
552 lute bias for annual mean maximum temperature is 0.58 K for the Noah-MP ensemble mean versus
553 1.18 K for the Noah-Unified ensemble. In particular, cold bias magnitudes for maximum temperature
554 are considerably lower over eastern and southern regions for the RCMs using Noah-MP (Figure 4d).
555 RMSE magnitudes for maximum temperature are substantially reduced over the topographically com-
556 plex regions of the southeast, and southwest and central regions (Figure 5d).

557 Overall, the magnitude of warm biases for minimum temperature are broadly similar for
558 Phase I and Phase II RCMs (Figure 4b,c). Conversely, while RCMs in both Phases show large
559 RMSEs for minimum temperature over several eastern regions, RMSEs are smaller for the Noah-MP
560 ensemble over some southern areas (Figure 5b,c).

561 In contrast to the above results for the simulation of maximum temperature, overall, Phase II
 562 RCMs using Noah-MP show smaller performance improvements for the simulation of precipitation
 563 relative to the Phase I RCMs (Table 7). However, precipitation bias magnitudes are smaller for the
 564 Noah-MP ensemble over specific regions, e.g., north-eastern coastal regions and the elevated terrain
 565 of the south-east (Figure 4c,f).

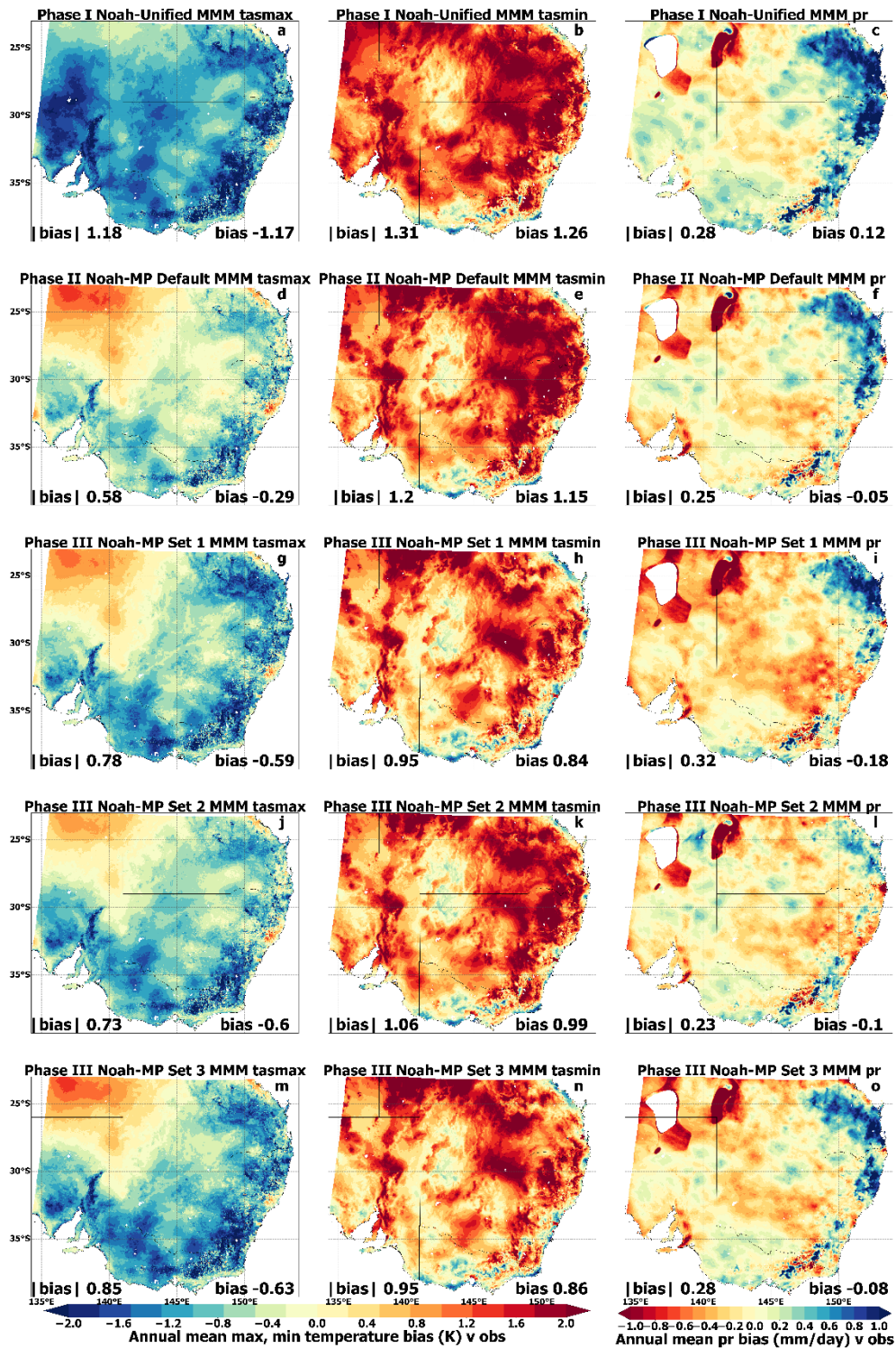
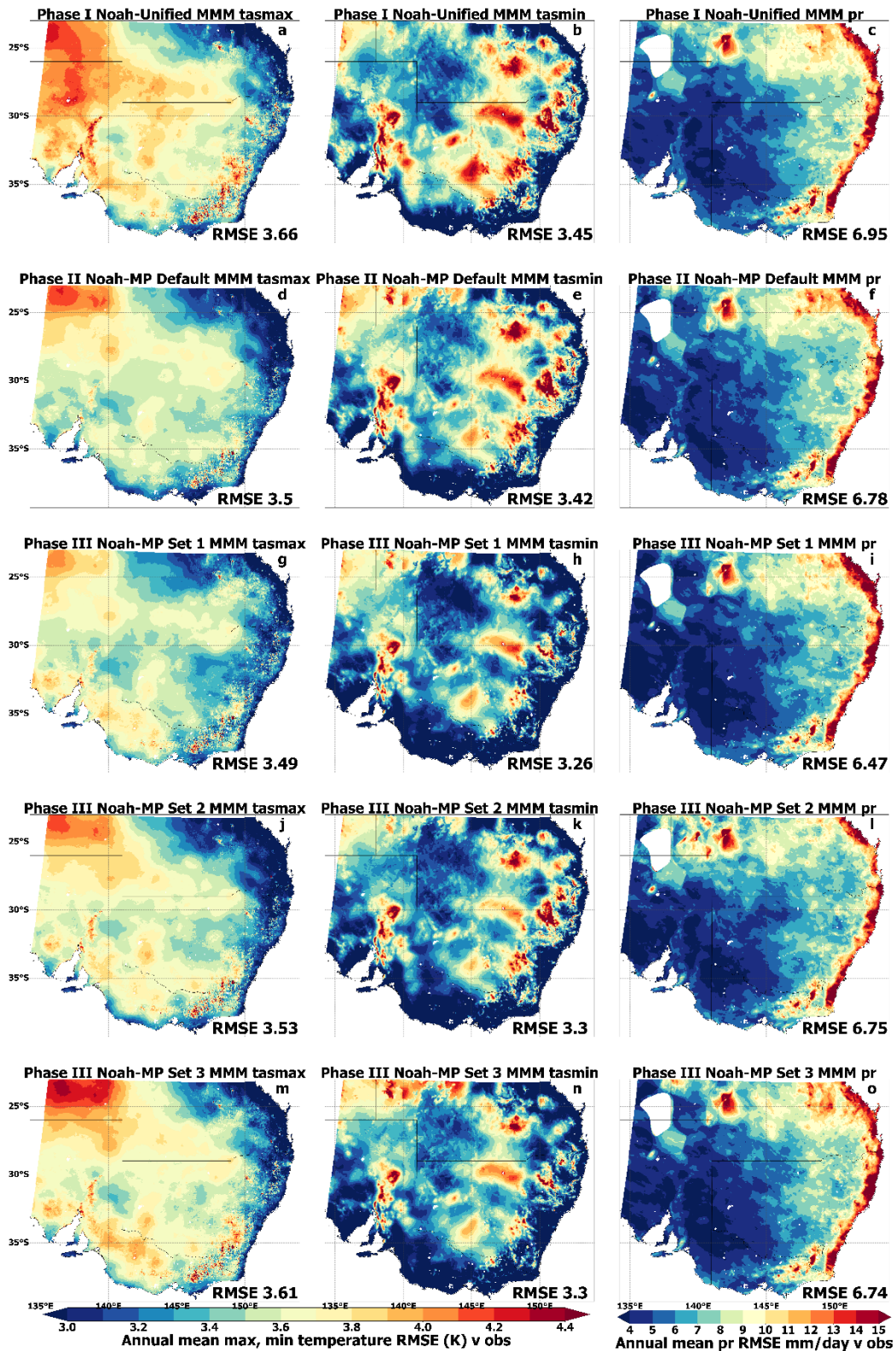


Figure 4. Phase I (N=36), Phase II (N=60) and Phase III (N=78) ensemble mean biases for annual mean maximum temperature, minimum temperature and precipitation with respect to Australian Gridded Climate Data

569 (AGCD) observations for NARClim 2.0 Phase I physics test RCMs using Noah-Unified as the land surface
 570 model (LSM) (a-c); Phase II physics test RCMs using Noah-MP as the LSM and its default settings (d-f); Phase
 571 III set 1 physics test RCMs using Noah-MP with dynamic vegetation cover activated (g-i); Phase III set 2 phys-
 572 ics test RCMs using Noah-MP with TOPMODEL surface runoff and simple groundwater activated (j-l); and
 573 Phase III set 3 physics test RCMs using Noah-MP with both dynamic vegetation cover and TOPMODEL runoff
 574 activated (m-o).



575

576 **Figure 5.** As per Figure 4 but showing RMSEs.

577 **5.2.2. Climate Extremes**

578 Climate extreme analysis assesses RCM representations of the hottest and the wettest day versus
 579 AGCD. For both extremes and for RCM biases and RMSEs, Phase II RCMs using NG radiation
 580 showed inferior performance relative to phase I RCMs using RRTMG (Table 8). Conversely, Phase II
 581 RCMs using Noah-MP show substantial reductions in bias for both the hottest and wettest days (Table
 582 8). Phase II Noah-MP RCMs show a small increase in RMSE for the hottest day (Phase I bias=3.59
 583 K; Phase II bias=3.74 K); however, RMSEs are smaller for the wettest day (i.e., Phase I RMSE=19.20
 584 mm; Phase II RMSE=18.47 mm) (Table 8).

585 **Table 8** Climate extremes performance: comparing phase I RCMs (N=12) with phase II RCMs (i.e.,
 586 12 RCMs changing radiation from RRTMG to New Goddard (NG) and 12 RCMs changing land sur-
 587 face model (LSM) from Noah-Unified to Noah-MP; NMP).

| Variable | Bias | | | RMSE | | |
|---------------------------|---------------------------------------|--|--|---------------------------------------|--|--|
| | Phase I (N=12) ensemble mean | Phase II (NG rad.) ensemble mean | Phase II (NMP LSM) ensemble mean | Phase I (N=12) ensemble mean | Phase II (NG rad.) ensemble mean | Phase II (NMP LSM) ensemble mean |
| Temp. max: hottest (K) | 1.11 | 1.93 | 0.81 | 3.59 | 3.97 | 3.74 |
| Prec.: wettest (mm) | 3.08 | 3.21 | 2.60 | 19.20 | 20.52 | 18.47 |

588 **5.3 Phase III RCM performance summary and shortlisting N=7 RCMs for** 589 **ERA5-NARClIM 2.0 evaluation simulations**

590 Overall, RCM biases for mean maximum temperature do not show marked improvements once the
 591 dynamic vegetation cover and surface runoff options are activated for Noah-MP (Figure 4 g,j,m) rela-
 592 tive to RCMs using Noah-MP with default settings (Figure 4d). However, specifically for the RCM
 593 ensemble with dynamic vegetation cover activated for Noah-MP, RMSE magnitudes for maximum
 594 temperature are lower over some eastern coastal regions (Figure 5g).

595 The simulation of mean minimum temperature shows clear performance improvements for
 596 Phase III RCMs using options activated for Noah-MP, relative to RCMs using Noah-MP defaults.
 597 Overall, both biases and RMSEs for minimum temperature are reduced in magnitude for RCMs using
 598 either or both of dynamic vegetation cover and runoff/groundwater options activated for Noah-MP,

599 relative to the default parameters (Figure 4-5). These performance improvements are largest over
600 eastern and southern regions.

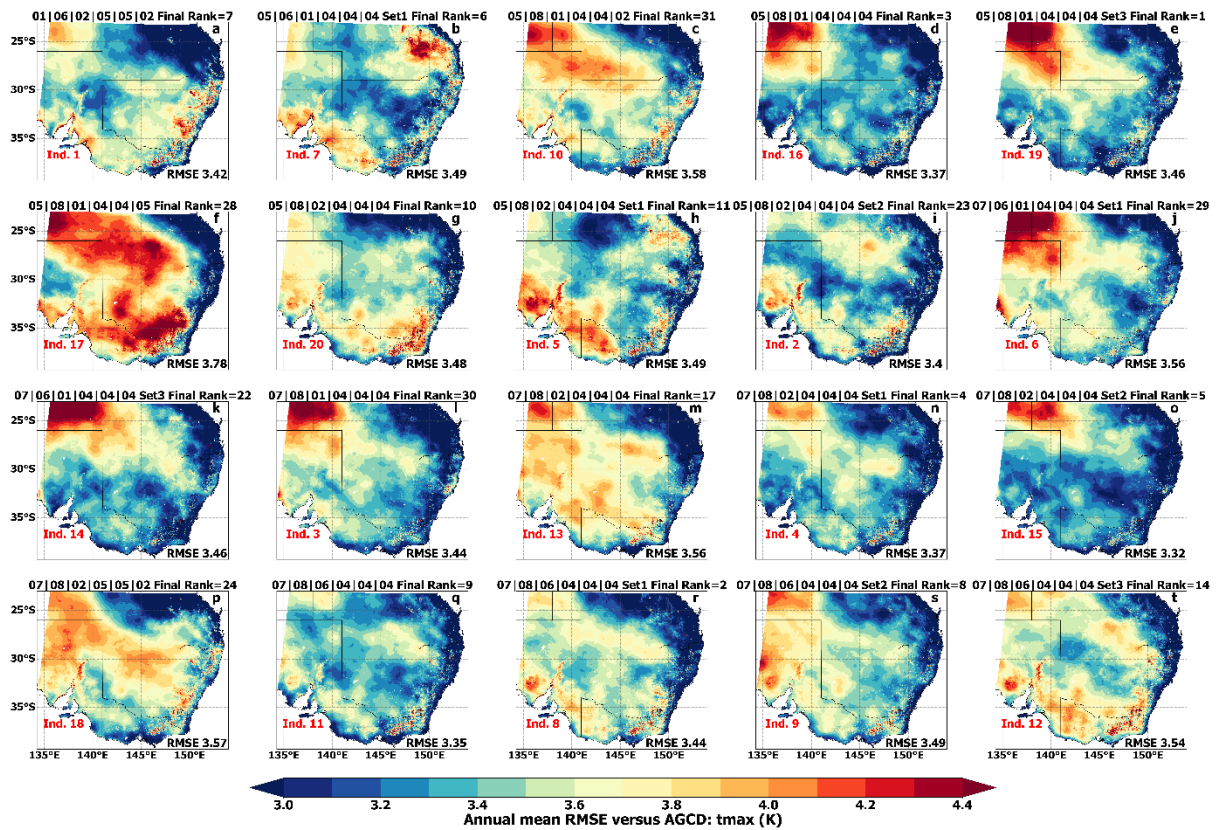
601 There are no substantial overall performance improvements in the simulation of precipitation
602 for Phase III RCMs relative to Phase II RCMs (Figures 4-5 f,i,l,o). However, using Noah-MP with
603 specific LSM options remains favourable to using RCMs with Noah-Unified, albeit the performance
604 gains are generally small, except for some coastal regions and especially the north-east.

605 All 78 RCMs in the complete RCM physics test ensemble are ranked for performance as de-
606 scribed in Sect. 3.2. Once the poor-performing RCMs are excluded, there are 20 RCMs remaining
607 (Table 9; Figures 6-8). In Table 9, we see that 16 Noah-MP-based RCMs from Phase II and Phase III
608 comprise this set of 20 RCMs, with 3 of the 20 RCMs using Noah-Unified, and 1 using CLM4.0. For
609 maximum temperature, some shortlisted RCMs show substantial RMSEs over north-western and in-
610 land areas (e.g., Figure 6 d-f) that are of larger magnitude over these areas than the ensemble means of
611 Phase I-III RCMs (Figure 5). Conversely, several shortlisted RCMs show very low RMSEs for maxi-
612 mum temperature across eastern and southern regions, especially along the eastern coast (Figure 6,
613 e.g., RCMs in panels d,l,n,o,q). For minimum temperature, a subset of the twenty shortlisted RCMs
614 show substantially reduced RMSEs over many regions relative to the Phase I-III ensemble means
615 (Figure 7, e.g., RCMs in panels: b,h,i). Additionally, several shortlisted RCMs show reduced RMSEs
616 for precipitation over the eastern coast and north-east (Figure 8, e.g., RCMs in panels: c, l, m, n, o)
617 relative to the Phase I-III RCM ensemble means in Figure 5c,f,i,l,o.

618 These 20 RCMs are assessed for statistical independence and 7 RCMs from this RCM set are
619 shortlisted for the ERA5-forced RCM simulations considering both their performance and independ-
620 ence scores (Table 9). These 7 shortlisted RCMs are listed in **bold** in Table 9 and are identified as R1-
621 R7 in the ERA5-forced evaluation simulations (Table 9; final column). RCMs are shortlisted from the
622 set of 20 if they rank highly for both performance and independence. For instance, RCM
623 050801040404_set_3 (top row, Table 9) is top-ranked for performance, however, its independence
624 scores/ranks are low, hence it is not shortlisted. It is important to note that, while a general perfor-
625 mance gain is observed in the physics testing when using Noah-MP, there are some specific RCM
626 configurations using Noah-Unified that perform well in simulating the Australian climate. For in-
627 stance, the RCM 010602050502 (row 7; Table 9; R1) uses Noah-Unified and performs well overall
628 (its overall performance rank=7), and especially for the simulation of maximum temperature (Figure
629 6a). It is also the only RCM in this set of 20 RCMs to use YSU for PBL. Importantly, this RCM is
630 highly ranked for statistical independence, hence, this RCM is shortlisted for the N=7 set. We note
631 here that R1-R7 are simply a chronological naming convention and do not imply any ranking for these
632 7 RCM configurations.

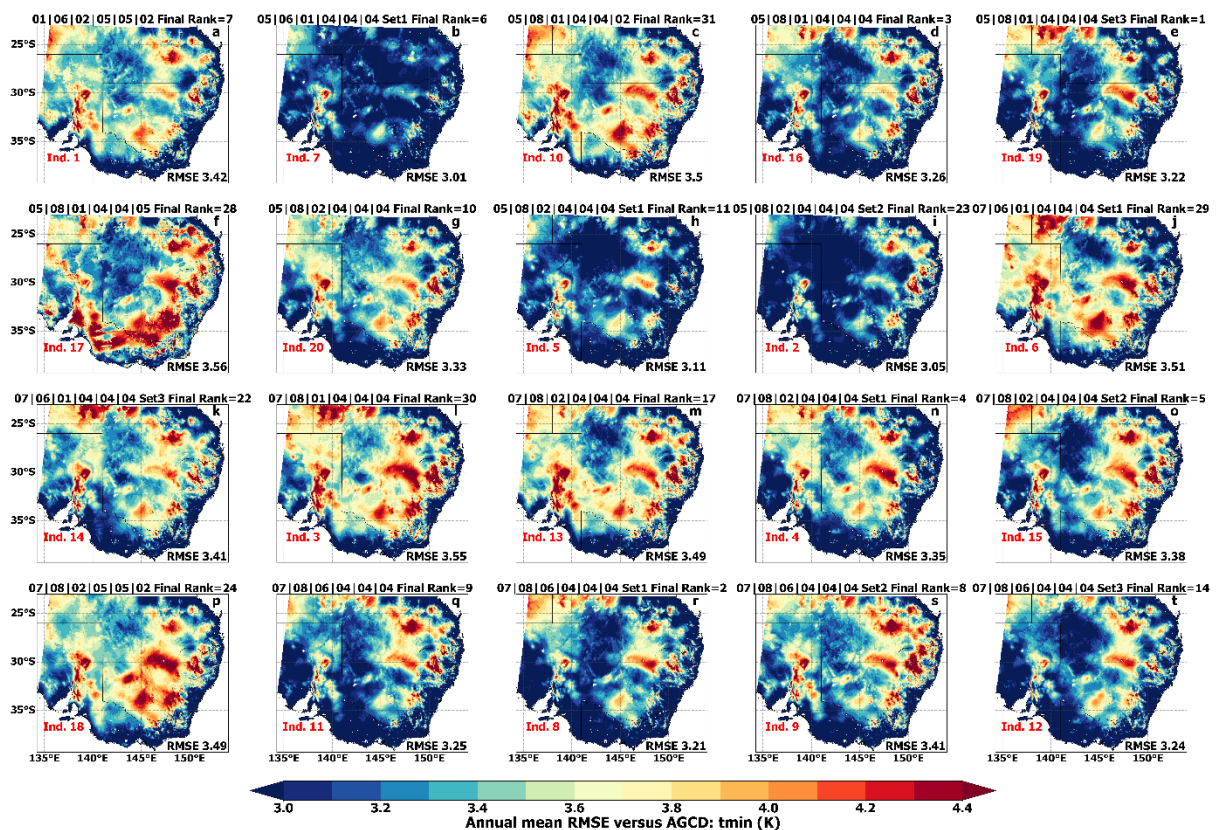
633 **Table 9.** The 20 NARClIM 2.0 physics test RCMs shortlisted from the ensemble of 78 RCMs based on their
634 performance in simulating the Australian climate and independence (Ind.). N=7 R1-R7 RCMs shortlisted for
635 ERA5-forced evaluation simulations shown in **bold**. R1-R7 are a naming convention and do not imply a ranking
636 for these 7 RCMs. NU=Noah Unified; NMP=Noah-MP; DV=dynamic vegetation cover; TOP=topmodel runoff.

| # | RCM Physics Combination | PBL | MP | Cumulus | SW/LW | LSM | Test Phase | Overall Performance Rank | Bishop Abramowitz Ind. Rank | Herger Ind. Set 1 | Herger Ind. Set 2 | ERA5-forced RCM Identifier |
|---|---------------------------|--------------|-------------|------------|--------------|----------------|------------|--------------------------|-----------------------------|-------------------|-------------------|----------------------------|
| 1 | 050801040404_set_3 | MYNN2 | Thom | KF | RRTMG | NMP DV+TOP | III | 1 | 19 | 20 | 20 | |
| 2 | 070806040404_set_1 | ACM2 | Thom | Td | RRTMG | NMP DV | III | 2 | 8 | 5 | 6 | R6 |
| 3 | 50801040404 | MYNN2 | Thom | KF | RRTMG | NMP | II | 3 | 16 | 12 | 13 | |
| 4 | 070802040404_set_1 | ACM2 | Thom | BMJ | RRTMG | NMP DV | III | 4 | 4 | 3 | 3 | R5 |
| 5 | 070802040404_set_2 | ACM2 | Thom | BMJ | RRTMG | NMP TOP | III | 5 | 15 | 13 | 12 | |
| 6 | 050601040404_set_1 | MYNN2 | WSM6 | KF | RRTMG | NMP DV | III | 6 | 7 | 10 | 10 | R2 |
| 7 | 10602050502 | YSU | WSM6 | BMJ | NG | NU | II | 7 | 1 | 3 | 3 | R1 |
| 8 | 070806040404_set_2 | ACM2 | Thom | Td | RRTMG | NMP TOP | III | 8 | 9 | 9 | 5 | R7 |
| 9 | 70806040404 | ACM2 | Thom | Td | RRTMG | NMP | II | 9 | 11 | 14 | 14 | |
| # | 50802040404 | MYNN2 | Thom | BMJ | RRTMG | NMP | II | 10 | 20 | 19 | 19 | |
| # | 050802040404_set_1 | MYNN2 | Thom | BMJ | RRTMG | NMP DV | III | 11 | 5 | 2 | 2 | R3 |
| # | 070806040404_set_3 | ACM2 | Thom | Td | RRTMG | NMP DV+TOP | III | 14 | 12 | 10 | 10 | |
| # | 70802040404 | ACM2 | Thom | BMJ | RRTMG | NMP | II | 17 | 13 | 15 | 15 | |
| # | 070601040404_set_3 | ACM2 | WSM6 | KF | RRTMG | NMP DV+TOP | III | 22 | 14 | 16 | 16 | |
| # | 050802040404_set_2 | MYNN2 | Thom | BMJ | RRTMG | NMP TOP | III | 23 | 2 | 4 | 4 | R4 |
| # | 70802050502 | ACM2 | Thom | BMJ | NG | NU | II | 24 | 18 | 18 | 18 | |
| # | 50801040405 | MYNN2 | Thom | KF | RRTMG | CLM4 | I | 28 | 17 | 17 | 17 | |
| # | 070601040404_set_1 | ACM2 | WSM6 | KF | RRTMG | NMP DV | III | 29 | 6 | 7 | 8 | |
| # | 70801040404 | ACM2 | Thom | KF | RRTMG | NMP | II | 30 | 3 | 1 | 1 | |
| # | 50801040402 | MYNN2 | Thom | KF | RRTMG | NU | I | 31 | 10 | 6 | 7 | |



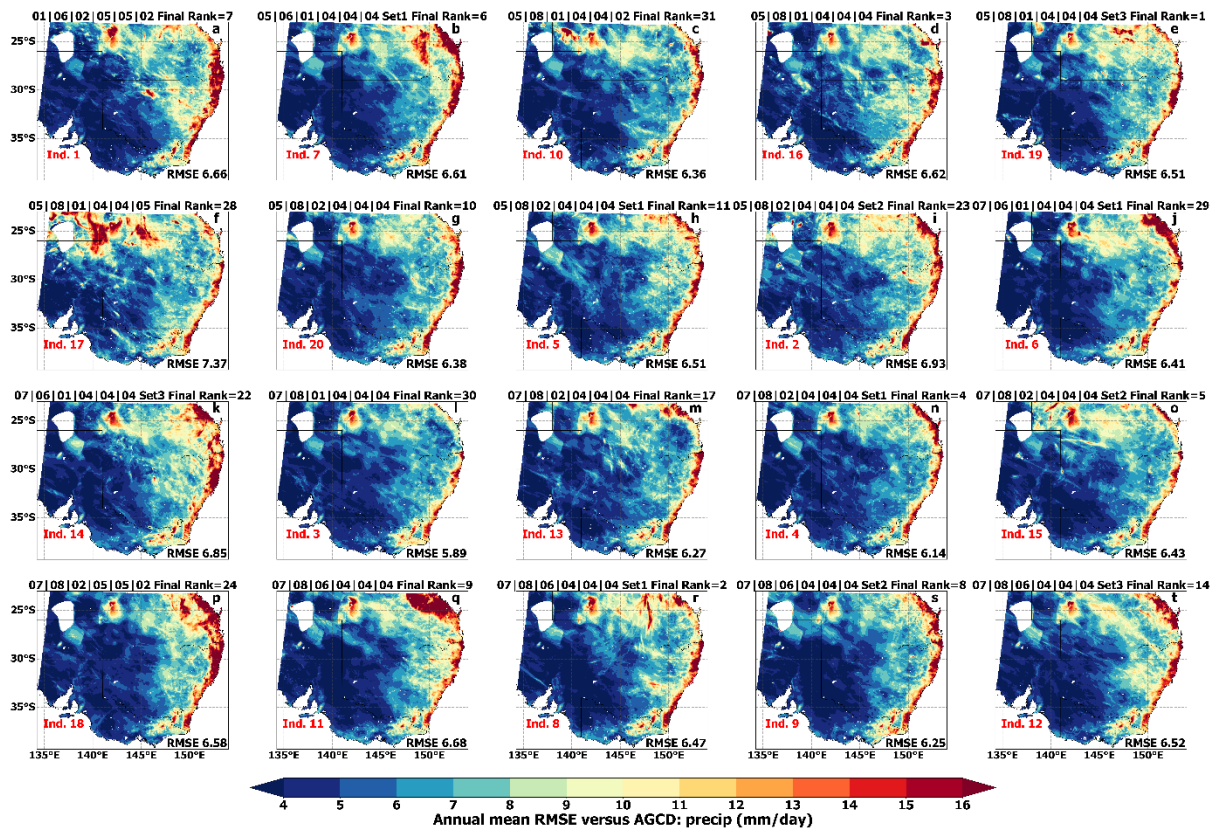
637

638 **Figure 6.** RMSEs for modelled mean maximum temperature (tmax) versus observations for the twenty
 639 NARCIIM 2.0 physics test RCMs shortlisted from the full ensemble of seventy-eight RCMs based on their
 640 performance in simulating the recent south-east Australian climate. Overall (final) performance ranks and
 641 Bishop and Abramowitz (2013) method independence (Ind.) scores are shown.



642
643

Figure 7. As per Figure 6 but for mean minimum temperature (tmin).



644

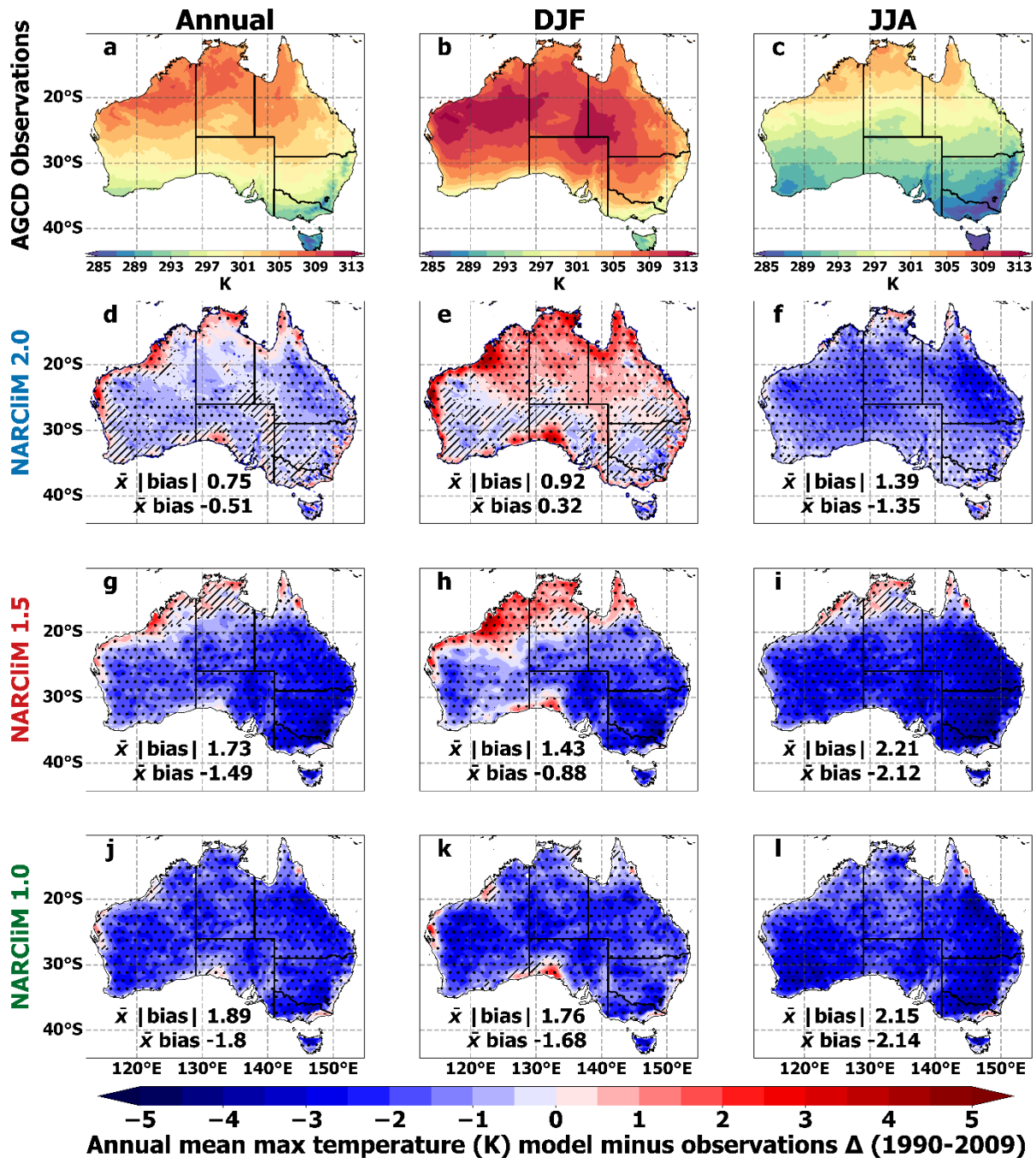
645 **Figure 8.** As per Figure 6 but for mean precipitation (precip.).

646 **6. CORDEX-CMIP6 NARClIM 2.0 historical evaluation**

647 **6.1 Maximum temperature**

648 Overall, NARClIM 2.0 RCMs simulate maximum temperature more accurately than NARClIM1.x,
 649 with widespread, statistically significant reductions in cold biases in the ensemble mean (Figure 9), as
 650 well as for many individual RCMs (Supporting Information Figure S4-S6). These reductions in bias
 651 apply for all timescales but are largest for the annual mean, i.e., the area-averaged mean absolute bias
 652 for the NARClIM 2.0 ensemble is 0.75 K (range: 0.61 to 2.03 K), 1.73 K (range: 1.1 to 2.37 K) for
 653 NARClIM 1.5, and 1.89 K (range: 0.55 to 4.12 K) for NARClIM 1.0 (Figure 9d,g,j and Figure S4).
 654 Notably, the NARClIM2.0 ensemble mean annual mean maximum temperature bias magnitudes are
 655 small, i.e., around <0.5 K, over south-west WA, southern coastal regions, and several eastern regions.
 656 This may be important from a climate change adaptation and mitigation perspective as these regions
 657 are heavily populated and economically significant. NARClIM 2.0 retains warm biases of similar
 658 magnitude to NARClIM 1.5 along the north-west coast of Australia (Figure 9d,g). Moreover, these
 659 warm biases cover additional areas for NARClIM 2.0, especially during DJF (Figure 9e,h). A wide
 660 range of bias signs are evident for the individual NARClIM 2.0 ensemble members (Figures S4-S6)
 661 and a minority of NARClIM 2.0 RCMs retain strong cold biases, e.g., at an annual timescale NAR-

662 CliM 2.0-NorESM2-MM R3 (mean absolute bias = 2.03 K) and UKESM-1-0-LL R3 (1.77 K). Addi-
 663 tionally, the R5 RCM is generally warmer than R3 (e.g., Figure S4c,d). Considering the forcing GCM
 664 data, overall, ensemble means for the CMIP6 and CMIP5 GCMs generally show similar patterns and
 665 magnitudes of cold bias for maximum temperature (Supporting Information S7).



666

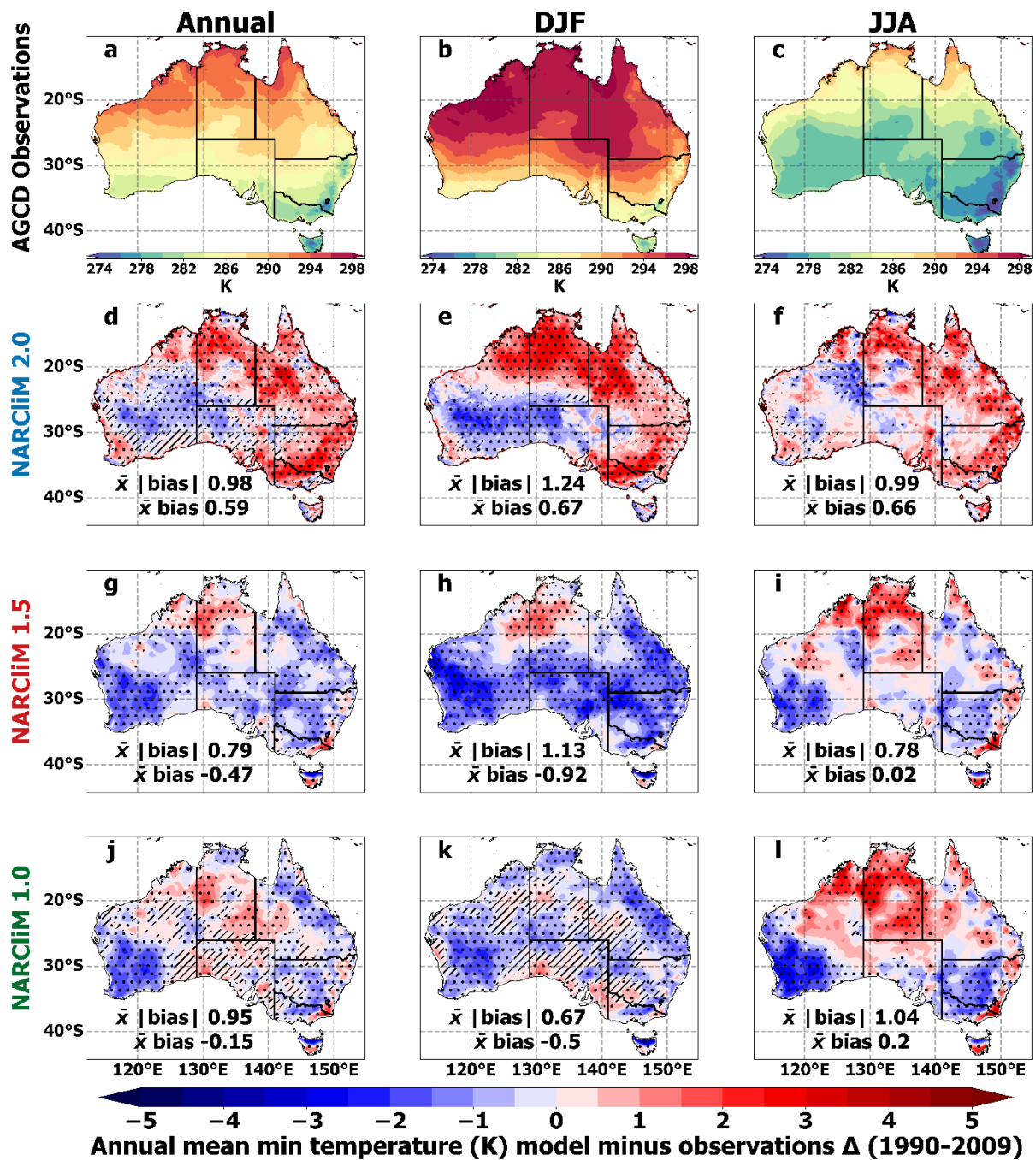
667 **Figure 9.** Annual, DJF and JJA mean near-surface atmospheric maximum temperature biases for NARCIiM 2.0,
 668 1.5 and 1.0 historical ensemble means with respect to Australian Gridded Climate Data (AGCD) observations
 669 for 1990-2009. Stippled areas indicate locations where an RCM shows statistically significant bias. Significance
 670 stippling for the ensemble mean bias follows Tebaldi et al. (2011) and is applied separately to each RCM en-
 671 semble. Statistically insignificant areas are shown in colour, denoting that less than half of the models are signi-
 672 ficantly biased. In significant agreeing areas (stippled), at least half of RCMs are significantly biased, and at least

673 70% of significant RCMs in each ensemble agree on the direction of the bias. Significant disagreeing areas are
674 shown in hatching, which are where at least half of the models are significantly biased and less than 70% of
675 significant models in each ensemble agree on the bias direction - see main text for additional detail on the stip-
676 pling regime.

677 **6.2 Minimum temperature**

678 The simulation of mean minimum temperature by NARClIM 2.0 is generally warm biased at all time-
679 scales (Figure 10). Its bias magnitudes over many regions are larger versus NARClIM 1.5, e.g., annual
680 mean area-averaged absolute biases are 0.98 K and 0.79 K for NARClIM 2.0 and NARClIM 1.5, re-
681 spectively (Figure 10 d,g). However, there are exceptions to this result over specific regions, for ex-
682 ample, parts of south-west western Australia show annual mean bias magnitudes of <1 K for NAR-
683 ClIM 2.0, but these areas show biases below -2 K for NARClIM1.x (Figure 10d,g,j). Most individual
684 RCMs comprising the NARClIM 2.0 ensemble show stronger warm biases than their NARClIM 1.5
685 peers at both annual and seasonal timescales (Figures S8-S10). The ACCESS-ESM-1-5-forced NAR-
686 ClIM 2.0 RCMs are considerably more warm-biased than the other NARClIM 2.0 RCMs, with aver-
687 age absolute biases of 1.74 K and 1.9 K; Fig. S8c-d).

688 Many of the CMIP6 GCMs used to force the NARClIM 2.0 RCMs are warmer than the CMIP5
689 GCMs used to force NARClIM 1.5, such that the ensemble mean bias of the former is 1.9 K versus
690 1.11 K (Figure S11). In particular, ACCESS-ESM-1-5 and MPI-ESM1-2-HR are substantially more
691 warm-biased relative to all other selected GCMs, with mean absolute biases of 2.2K and 3.47K, re-
692 spectively (Figure S11). This suggests that NARClIM 2.0's warm biases for mean minimum tempera-
693 ture are at least partially inherited from the driving data. However, whilst the ACCESS-ESM-1-5-
694 forced NARClIM 2.0 RCMs are much warmer than their counterparts (i.e., 1.74 K and 1.9 K), this
695 does not apply to the MPI-ESM1-2-HR-forced RCMs, which have biases of only 1.01 K and 1.09 K.
696 Hence, factors additional to the driving data, such as changes in RCM parameterisations between
697 NARClIM generations and other model design changes likely contribute to the warmer biases ob-
698 served for NARClIM 2.0.



699

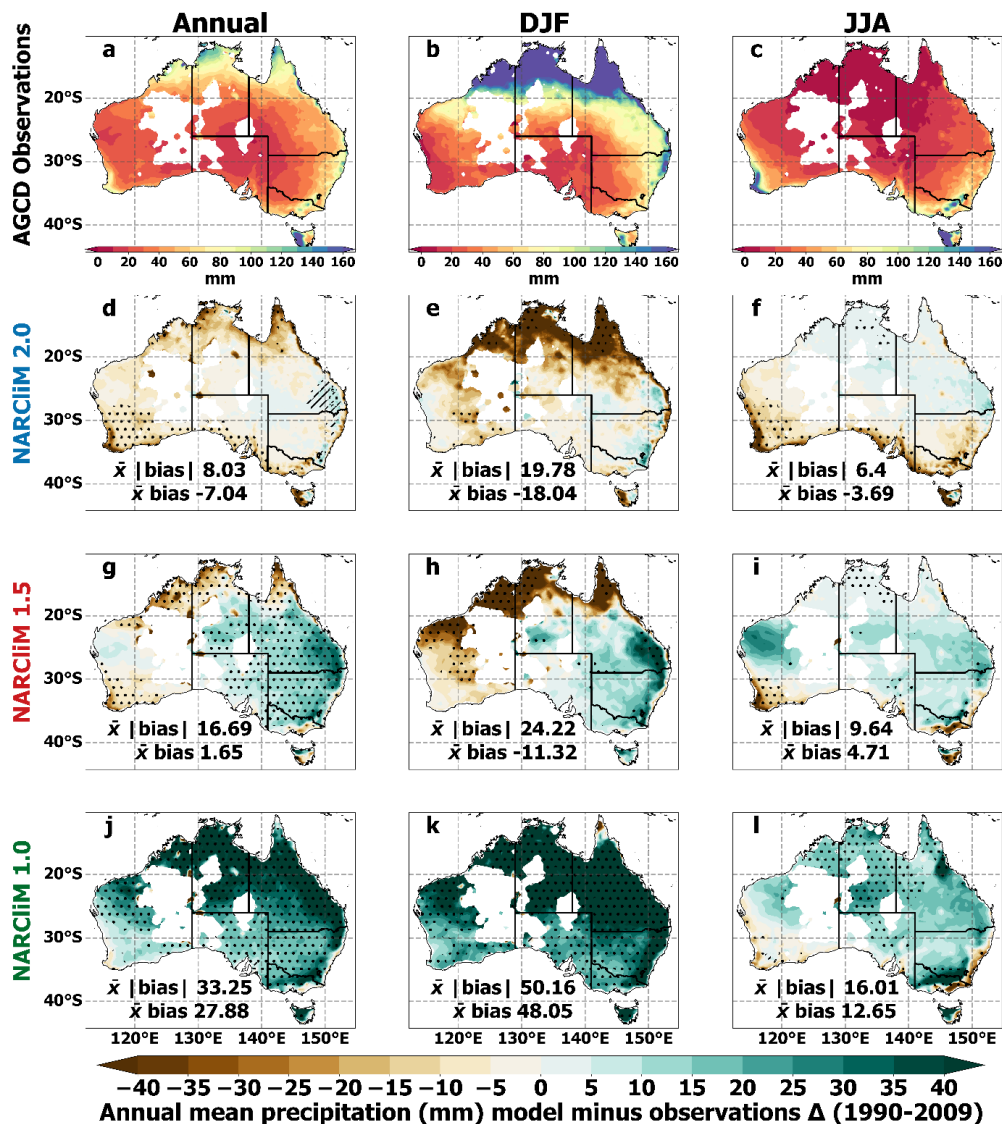
700 Figure 10. As per Figure 9 but for mean minimum temperature.

701 6.3 Precipitation

702 The NARCIIM 2.0 ensemble shows small dry biases for mean precipitation over most regions, except
 703 for some areas mainly in the east of the country which show slight wet biases (Figure 11d-f). This
 704 contrasts with stronger wet biases of NARCIIM 1.5 that are statistically significant over many regions
 705 (Figure 11g-i) and the even stronger wet biases of NARCIIM 1.0 (Figure 11j-l). Area-averaged bias
 706 magnitudes are considerably smaller for NARCIIM 2.0 relative to NARCIIM1.x, especially for the
 707 annual mean, i.e., 8.03 mm versus 16.69 mm and 33.25 mm, respectively. Annual mean precipitation

708 biases are particularly small over eastern regions, often being <5 mm. NARClIM 2.0 retains the strong
 709 summertime dry biases for precipitation over northern Australia that are also evident for NARClIM
 710 1.5 (Figure 11e,h), noting that this region also shows strong warm biases for maximum temperature
 711 (Figure 9).

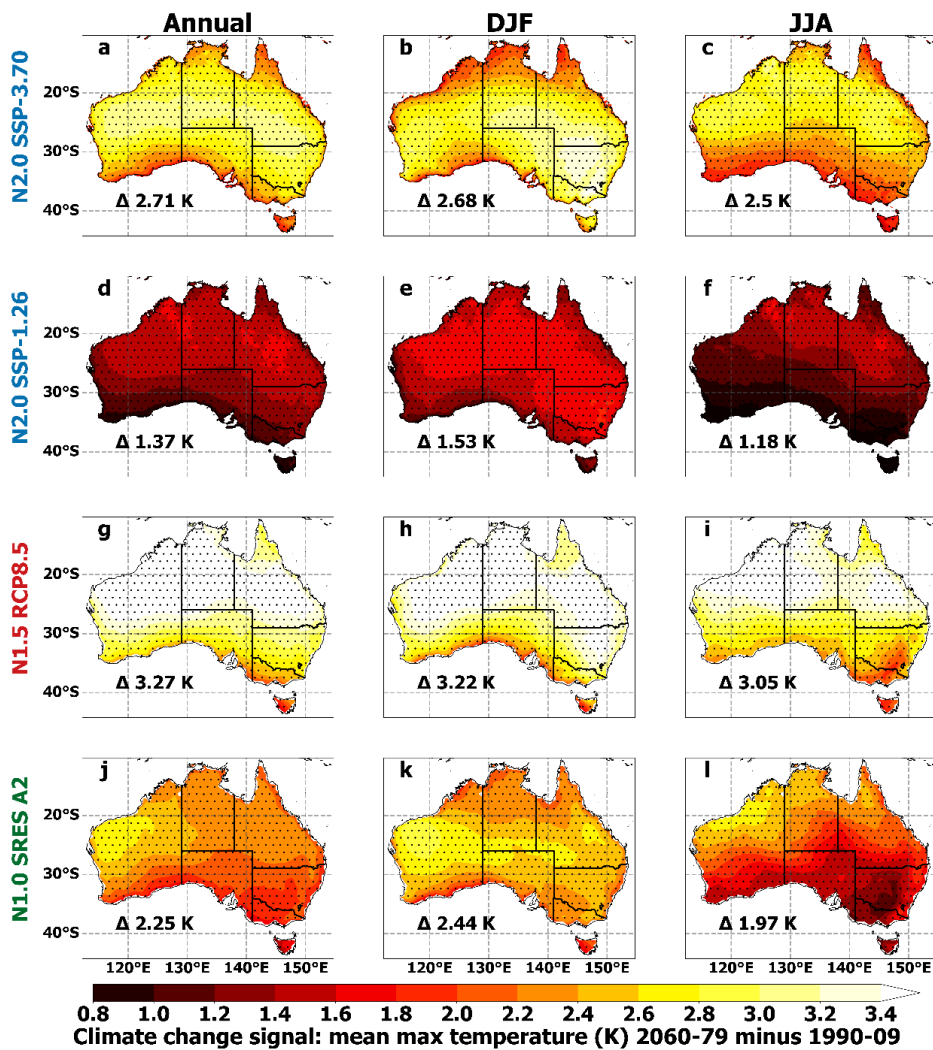
712 The individual RCMs comprising NARClIM 2.0 show a range of results for annual and sea-
 713 sonal mean precipitation biases (Fig S12-S14). Notably, three of the ten NARClIM 2.0 RCMs have
 714 substantially larger bias magnitudes than their peers at annual and summer timescales, i.e., both MPI-
 715 ESM1-2-HR-R3 and R5 (absolute biases are 15.53 mm and 22.45 mm for annual mean precipitation,
 716 Figure S12g-h) and EC-Earth3-Veg-R5 (Figure S12f; 18.59 mm). Despite EC-Earth3-Veg-R5 being
 717 strongly dry-biased, EC-Earth3-Veg-R3 simulates precipitation more accurately i.e., its mean absolute
 718 bias=9.53 mm (Figure S12e). Analogously to NARClIM 2.0's performance for temperature, R5 is
 719 drier than R3. Comparing the ensemble means of the driving GCMs, the CMIP6 GCMs are marginal-
 720 ly more accurate in simulating annual mean precipitation than the CMIP5 GCMs (Figure S15). Whilst
 721 the CMIP6 ensemble produces small biases over inland areas, its biases are larger along the east coast.



722
 723 **Figure 11.** As per Figure 9 but for mean precipitation (precip.).

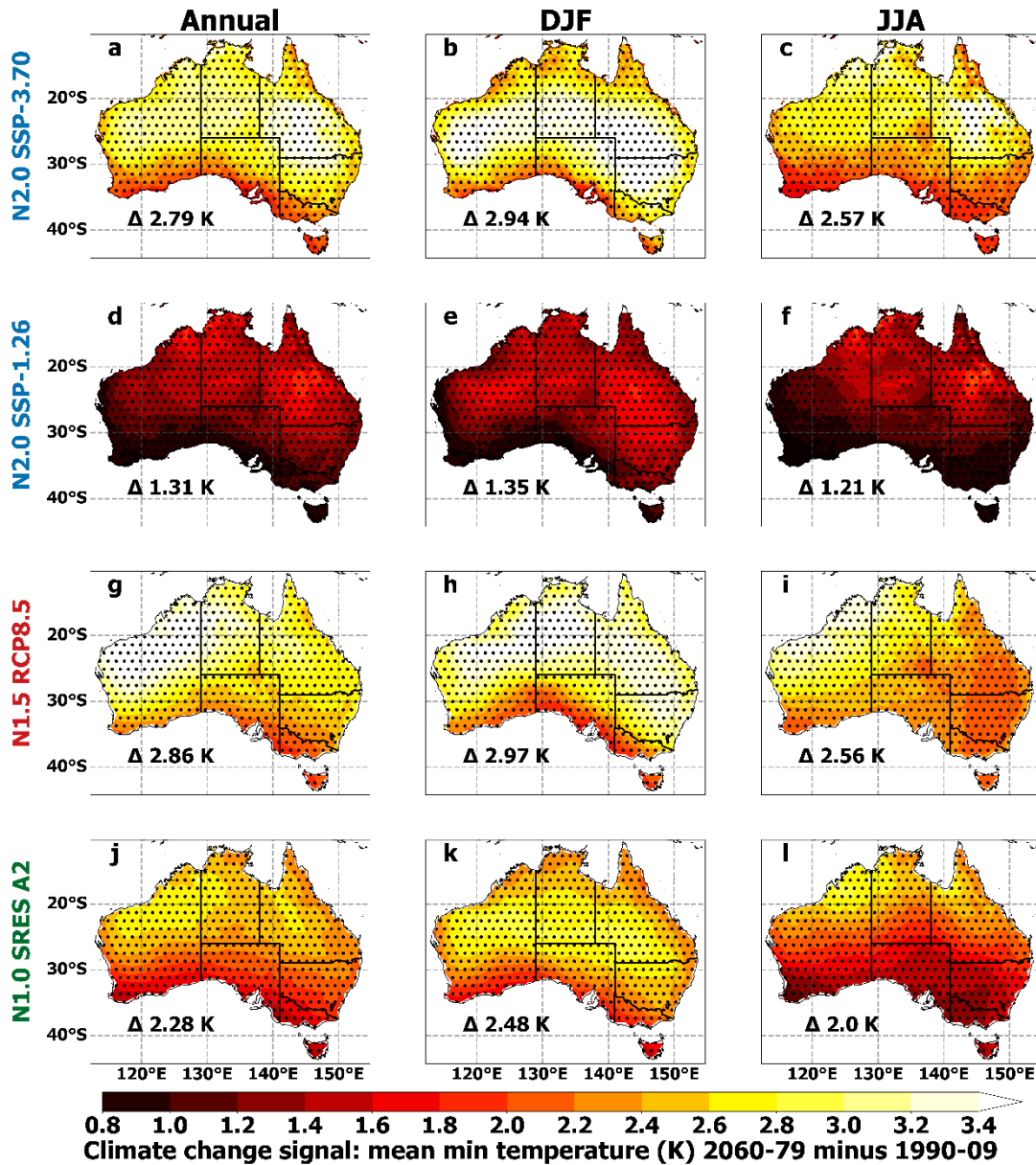
724 **7. CORDEX-CMIP6 NARClM 2.0 climate change projections**

725 Dependent on location, the largest maximum temperature projected increases for NARClM 2.0 under
 726 SSP3-7.0 are over ~3 K, and over ~1.5 K under SSP1-2.6 (Figure 12a,d). SSP3-7.0-NARClM 2.0
 727 shows faster warming over inland than coastal regions, with greater warming across a horizontal band
 728 of the continent during annual and summer timescales (Figure 12a-b). This contrasts with NARClM
 729 1.5 which shows a north-south warming gradient at annual and seasonal timescales, with its fastest
 730 warming rate over northern regions, and NARClM 1.0 which projects fastest warming over the west
 731 (Figure 12). For NARClM 2.0, the tropical north warms faster during the winter dry season than dur-
 732 ing the summer wet season under SSP3-7.0, but this is not the case for SSP1-2.6 (Figure 12b-c; e-f).
 733 NARClM 2.0 simulations under SSP3-7.0 show less warming than NARClM 1.5-RCP8.5, but
 734 warmer futures than for NARClM 1.0-SRES A2, with differences in the underlying driving GCMs
 735 and GHG scenarios likely contributing to these variations in warming. As per NARClM1.x, all
 736 NARClM 2.0 maximum temperature projections are significant-agreeing with all RCMs projecting
 737 statistically significant temperature increases.



738
 739 **Figure 12.** Ensemble mean climate change projections (far future minus present-day) for annual, DJF and JJA
 740 mean maximum temperatures with significance stippling as per Figure 9.

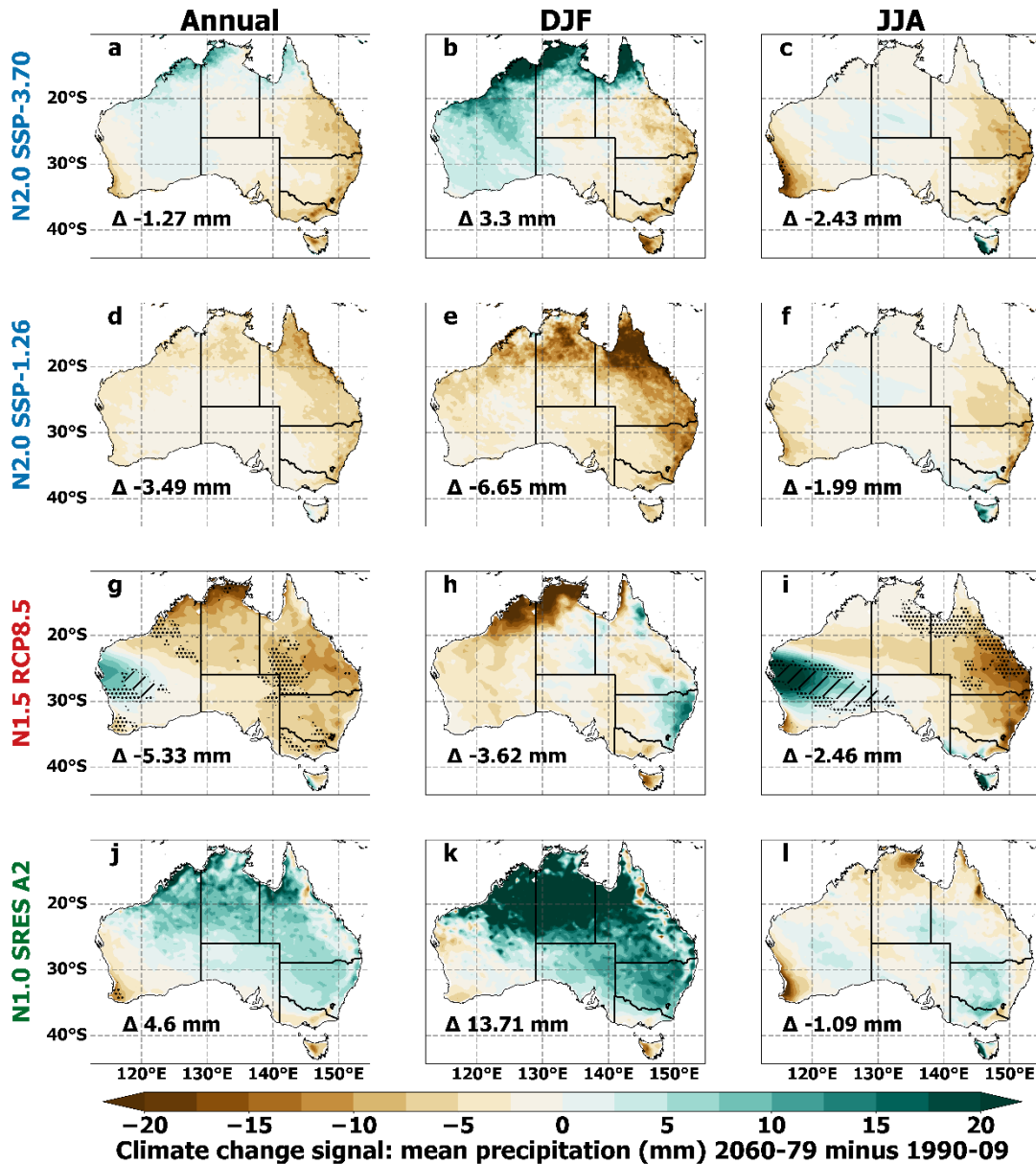
741 Projected increases in annual mean minimum temperature for NARcliM 2.0 exceed 3 K over
 742 some regions for SSP3-7.0, and 1.6 K for SSP1-2.6 (Figure 13). Under both GHG scenarios, at annual
 743 and winter timescales warming is fastest over north-east Australia. Conversely, NARcliM1.x mini-
 744 mum temperature future increases are generally largest over northwest or northern Australia, though
 745 the summertime projection for NARcliM 1.0 is an exception (Figure 13k). As for maximum tempera-
 746 ture projections, all RCMs for all NARcliM generations project statistically significant increases.



747
 748 **Figure 13.** Ensemble mean climate change projections (far future minus present-day) for annual, DJF and JJA
 749 mean minimum temperatures with significance stippling as per Figure 9.

750 NARcliM 2.0 SSP3-7.0 projects a dry future over most of Australia, except for wetter futures
 751 over northern and western regions, which are largest in magnitude in summer (Figure 14a-b). In con-
 752 trast, overall, NARcliM 2.0 SSP1-2.6 projects dry changes across most of Australia, with the strong-
 753 est drying over northern Australia during summer (Figure 14e). Similarities between NARcliM 2.0

754 projections for the low and high GHG SSPs include faster drying over the eastern coastline at all
 755 timescales, especially during summer. The wetter futures projected by RCMs downscaling SSP3-7.0-
 756 GCMs relative to SSP1-2.6 may be partially inherited from the driving CMIP6 GCMs, because over-
 757 all, SSP3-7.0 GCMs show wetter futures than corresponding SSP1-2.6 GCMs (Fig. S16).

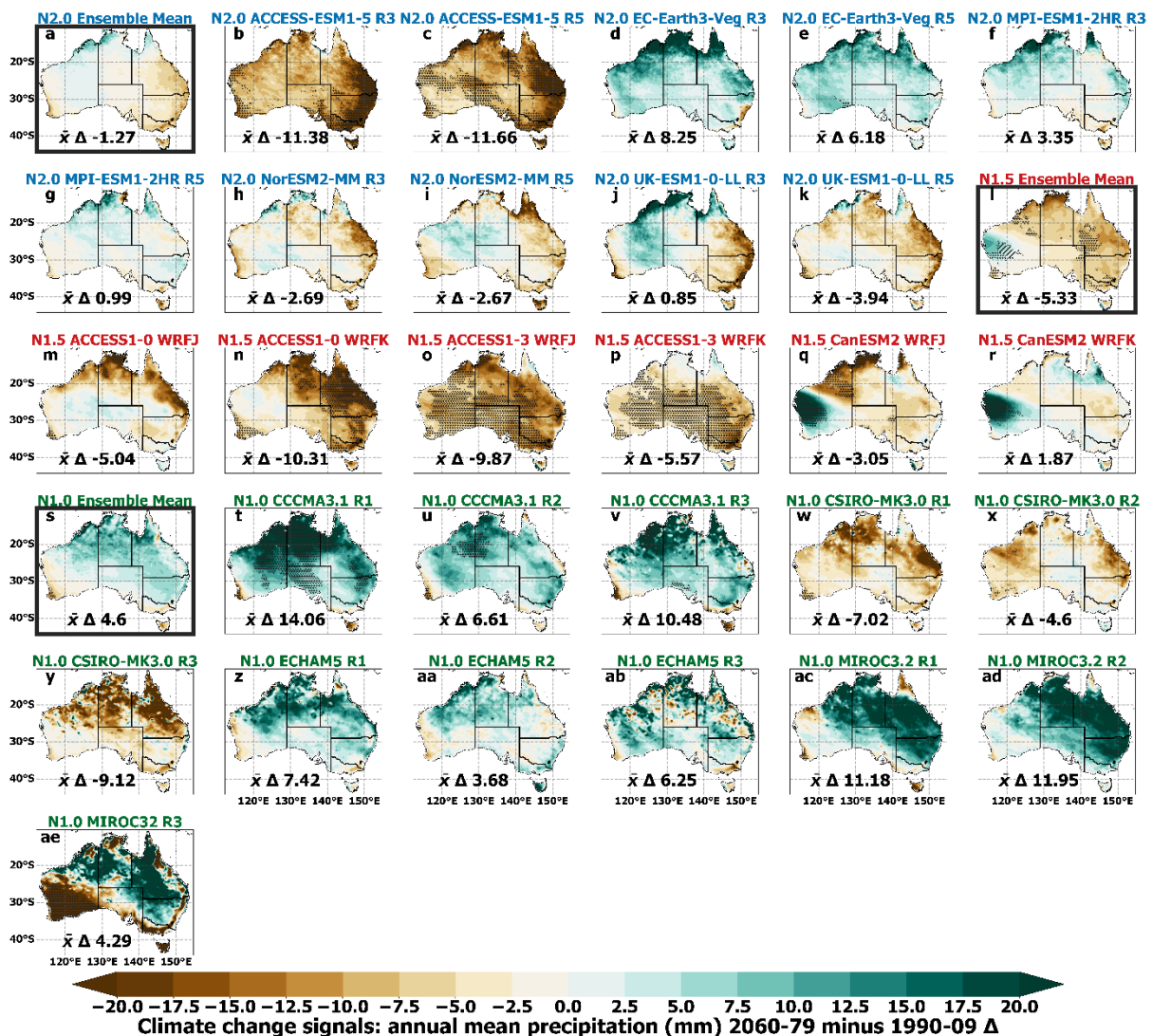


758
 759 **Figure 14.** Ensemble mean climate change projections (far future minus present-day) for annual, DJF and JJA
 760 mean precipitation with significance stippling as per Figure 9.

761 Considering mean precipitation projections for individual NARClIM 2.0 RCMs, in some cases,
 762 R3 and R5 RCMs produce similar results when downscaling the same GCM. For instance, ACCESS-
 763 ESM-1-5 forced R3 and R5 both show strong projected decreases in annual mean precipitation across
 764 Australia (Figure 15b-c). In contrast, while UK-ESM1-0-LL R3-R5 both show projected decreases in
 765 annual mean precipitation over eastern Australia, R3 shows precipitation increases that are substan-
 766 tially more widespread over western and northern regions relative to R5 (Figure 15j-k). Overall, the

767 NARcliM 2.0 ensemble members show a variety of climate change signals for precipitation (Figure
 768 15) and temperature (not shown), reflecting the range within the larger CMIP6 ensemble (Di Virgilio
 769 et al. 2022).

770 There are some key differences between the mean precipitation projections of NARcliM 2.0 rel-
 771 ative to those of previous NARcliM generations. For instance, NARcliM 1.5 shows stronger reduc-
 772 tions in future precipitation over northern and eastern regions at annual and winter timescales (Figure
 773 14), and these changes are statistically significant over a few regions, whereas projected changes for
 774 NARcliM 2.0 are largely non-significant. Additionally, NARcliM 2.0 projects marked precipitation
 775 decreases along the south-east coast during summer, while NARcliM 1.5 shows the opposite result
 776 (Figure 14). NARcliM 1.0 generally projects wet futures across larger portions of Australia, especial-
 777 ly at annual and summer timescales.



778
 779 **Figure 15.** Climate change projections (1990-2009 versus 2060-2079) for annual mean precipitation for NAR-
 780 cliM ensemble mean climate change signals (a,l,s) and for individual ensemble members for each generation of
 781 NARcliM simulation (NARcliM 2.0 under SSP3-7.0, NARcliM 1.5 under RCP8.5 and NARcliM 1.0 under
 782 SRES A2). Significance stippling as per Figure 9.

783 **8. Discussion and Summary**

784 NARClIM regional climate models produce robust climate projections at spatial scales suitable for
785 local-scale climate change analysis and impact decision-making. The third and latest generation of
786 these regional climate models, NARClIM 2.0, encompasses several model design advancements over
787 its predecessors. A key aim of this paper is to describe how NARClIM 2.0 differs from its predeces-
788 sors and explain the rationale for these design decisions. We also characterise the improvements in
789 model skill in simulating the Australian climate relative to previous NARClIM generations, as well as
790 compare climate projections across NARClIM generations. The next section discusses aspects of
791 NARClIM2.0 RCM design and parameterisation in relation to previous studies before reviewing dif-
792 ferences in the model biases and the climate projections of the NARClIM 2.0 versus NARClIM 1.x
793 RCMs.

794 **8.1 NARClIM 2.0 RCM physics testing**

795 In addition to RCM design choices including increased resolution, and incorporation of convection-
796 permitting modelling and urban physics, a major change for NARClIM 2.0 relative to its predecessors
797 is to use new WRF RCM configurations which are selected via a large suite of physics tests. RCM
798 performance evaluations for the NARClIM 2.0 RCM physics testing focused on the 4 km resolution
799 convection-permitting domain which does not use a cumulus physics parameterisation. Notably, the 7
800 candidate shortlisted RCMs from the N=78 physics test ensemble used three different cumulus pa-
801 rameterisations for their outer domains, with 4 RCMs using BMJ, 2 RCMs using Tiedtke, and 1 using
802 Kain-Fritsch. This indicates that differences in the outer domain boundary conditions have key influ-
803 ences on the RCM performances in the convection-permitting domain.

804 Using the Noah-MP LSM in the NARClIM 2.0 RCM physics tests conferred overall RCM
805 skill improvements relative to RCMs using the Noah-Unified LSM, especially in terms of the simula-
806 tion of temperature. Although using Noah-MP also improved the simulation of precipitation in some
807 respects, these improvements were smaller relative to the gains for temperature, and improvements
808 were mainly located over coastal regions. The developers of Noah-MP suggest that some limitations
809 in the Noah-Unified LSM have been modified to better represent several parameters. These include
810 surface layer radiation balances, snow depth, soil moisture and heat fluxes, leaf area-rainfall interac-
811 tion, vegetation and canopy temperature distinction, drainage of soil, and runoff.

812 In the NARClIM2.0 physics testing, improvements in RCM skill were evident for Noah-MP
813 with default settings. Activating specific parameterisations for this LSM (i.e. dynamic vegetation cov-
814 er and surface runoff-simple groundwater) delivered comparatively smaller gains in RCM perfor-
815 mances. Some previous studies have found no overall benefit of using Noah-MP with default settings.
816 For instance, Imran et al. (2018) conducted an evaluation of WRF coupled with a variety of LSMs

817 including Noah-MP using its default settings. They simulated short-duration (~3-day) heatwaves in
818 Melbourne, Australia and observed larger temperature biases using Noah-MP relative to RCMs using
819 Noah-Unified and CLM4.0. However, their focus on specific short duration heatwave events over one
820 urban area was not intended as a comprehensive evaluation of Noah-MP's performance. Additionally,
821 several physics schemes used by these authors differed to those used in the NARClIM 2.0 physics
822 testing, i.e., they used: PBL=MYJ; microphysics=Thompson; cumulus=Grell3D; radia-
823 tion=RRTMG/RRTMG. Only Thompson microphysics and RRTMG radiation are used in the NAR-
824 ClIM 2.0 physics testing. WRF and Noah-MP versions also differed, i.e., Imran et al. used WRF3.6.1
825 and a Noah-MP version prior to 3.7, whereas NARClIM 2.0 uses WRF4.1.2 and Noah-MP version
826 4.1. Additionally, there are also several studies that have reported benefits of using Noah-MP with
827 default parameters relative to other LSMs for other regions globally e.g. Chen et al. (2014b), Chen et
828 al. (2014a) and Salamanca et al. (2018).

829 The NARClIM 2.0 physics testing found that the optimal LSM configuration for simulation of
830 minimum temperature used Noah-MP with dynamic vegetation cover activated, even though the per-
831 formance gain relative to Noah-MP with default settings was small. Constantinidou et al. (2020) ran
832 WRF coupled with four LSMs (Noah-Unified, Noah-MP, CLM and, Rapid Update Cycle) over the
833 Middle East North Africa CORDEX domain. They compared the performance of Noah-MP with dy-
834 namic vegetation cover turned on and off and found that air and land temperatures were best simulat-
835 ed using Noah-MP with dynamic vegetation cover activated.

836 In terms of other NARClIM2.0 RCM parameterisations, focusing on PBL, by the completion
837 of Phase I physics testing, only 3 of 12 RCMs shortlisted for further testing use the YSU scheme. By
838 the completion of Phase II testing, all remaining RCMs using YSU are discarded, with only RCMs
839 using PBL schemes other than YSU remaining (i.e., ACM2 and MYNN2). YSU PBL is a first-order
840 closure scheme that expresses turbulent mixing via mean variables rather than prognostic variables
841 (Hong et al., 2006). It is classed as a non-local scheme because it estimates turbulent mixing by small-
842 scale eddies as well as representing transport caused by convective large eddies. Two previous studies
843 evaluating convection permitting WRF simulations using different parameterisations that included
844 YSU for the PBL scheme found that, relative to other PBL schemes, YSU produced the highest bias
845 for simulated precipitation (Huang et al., 2023; Nuryanto et al., 2019). However, these studies focused
846 on different regions globally and used various experimental setups that are not directly comparable to
847 those used here. Hence, a separate study investigating sensitivities of the NARClIM 2.0 RCMs to the
848 different PBL schemes is currently underway.

849 **8.2 CORDEX-CMIP6 NARClIM 2.0 historical evaluation**

850 We characterised the improvements conferred by NARClIM 2.0 over its predecessors in simulating
851 the present-day Australian climate. NARClIM 2.0 simulates mean maximum temperature and precipi-

852 tation more accurately than NARClIM1.x. Specifically, NARClIM1.x has strong maximum tempera-
853 ture cold biases which are in keeping with other downscaling projects of the CMIP3-CMIP5 eras, e.g.,
854 (Andrys et al., 2016; Evans et al., 2020b), but these are substantially reduced in NARClIM 2.0. A con-
855 tributing cause of CMIP5-forced RCM cold biases of maximum temperature is their overestimation of
856 precipitation (Evans et al., 2020). This relationship was also noted in ERA-Interim forced RCMs of
857 this same modelling era (Di Virgilio et al. 2019). In NARClIM 2.0, the widespread wet biases that
858 characterise the NARClIM1.x RCMs are reduced in magnitude. NARClIM 2.0 produces smaller wet
859 biases over eastern Australia, and smaller dry biases elsewhere, except for Australia's tropical north.
860 This marked reduction in wet bias magnitudes is one plausible contributing factor for the reduction in
861 maximum temperature cold bias for the NARClIM 2.0 RCMs. The CMIP6 and CMIP5 GCMs used to
862 drive NARClIM 2.0 and 1.5 RCMs generally show similar magnitudes of maximum temperature cold
863 bias. This suggests that the underlying nature of the CMIP6 driving data is not a principal factor un-
864 derlying the observed improvements for NARClIM 2.0's simulation of maximum temperature. In fact,
865 the RCMs appear to have a substantial influence on the reduced maximum temperature biases.

866 That NARClIM 2.0 underestimates precipitation over tropical northern Australia during the
867 wet season (summer) to a similar degree of magnitude to the NARClIM 1.5 RCMs indicates that the
868 newer models still struggle to accurately capture the strength of the Australian monsoon. That NAR-
869 ClIM1.x strongly overestimates precipitation over south-eastern Australia whereas wet biases over
870 this region are reduced for NARClIM 2.0 indicates that the newer models may confer an improved
871 simulation of broad-scale processes associated with synoptic-scale systems interacting with the extra-
872 tropical storm track over Australia (Grose et al., 2019).

873 The extent to which NARClIM2.0's improved simulation of precipitation might be attributa-
874 ble to its driving data warrants consideration. Overall, the CMIP6 GCMs used to drive NARClIM 2.0
875 show marginally reduced wet biases versus the CMIP5 GCMs used for NARClIM1.5 (e.g. area-
876 averaged ensemble mean absolute biases are 7.13 mm and 8.89 mm, respectively; Supporting Infor-
877 mation Figure S15). This suggests that the underlying nature of the CMIP6 driving data might not be
878 the principal factor underlying the observed improvements for NARClIM 2.0's simulation of mean
879 precipitation. Conversely, in terms of RCM design features, the use of the Noah-MP LSM in the
880 NARClIM 2.0 RCM physics tests conferred overall RCM skill improvements relative to RCMs using
881 the Noah-Unified LSM for both mean precipitation and mean maximum temperature. As noted above,
882 the developers of Noah-MP suggest that some features of the Noah-Unified LSM have been modified
883 to better represent several parameters. The production NARClIM2.0 RCMs used Noah-MP, whereas
884 NARClIM1.x RCMs used Noah-Unified. Given these performance improvements observed for RCMs
885 using Noah-MP versus using Noah-Unified, it is plausible that the newer LSM contributes to the im-
886 proved NARClIM2.0 skill in simulating precipitation and maximum temperature, for instance, via
887 changing the land surface feedback (via soil moisture) to the simulation of precipitation. This possibil-
888 ity requires more extensive investigation via future studies.

889 More generally, the scope of the present study was to focus on an initial "first-order" evalua-
890 tion of mean precipitation rather than extremes of precipitation. However, clearly valuable research
891 can now be undertaken into evaluating the skill of NARClIM 2.0 in simulating extreme precipitation,
892 subdaily precipitation, etc, using NARClIM 2.0 20 km and 4 km data, noting these data are now pub-
893 licly available. A good avenue for further research is to assess the potential added value in simulating
894 extreme and subdaily precipitation at convection permitting scale versus the convection-parameterised
895 20 km data. Several previous studies have confirmed that convection-permitting resolution models
896 can improve the simulation of daily and sub-daily rainfall extremes (Xie et al., 2024; Cannon and
897 Innocenti, 2019; Kendon et al., 2017).

898 NARClIM 2.0 RCMs overestimate minimum temperatures across Australia, and these biases
899 are larger relative to NARClIM 1.5 but comparable to those of NARClIM 1.0. The CMIP6 GCMs
900 used to force NARClIM 2.0 show substantially stronger warm biases for minimum temperature than
901 the CMIP5 GCMs used for NARClIM 1.5. This suggests that the increased warm bias for minimum
902 temperature in NARClIM 2.0-RCMs could be partially inherited from the driving GCMs. However,
903 Noah-MP's simulation of factors such as LAI and other aspects of vegetation as well as surface albe-
904 do in semi-arid and arid areas has been shown to have deficiencies (Glotfelty et al., 2021). These is-
905 sues may contribute to some of the biases shown by the NARClIM 2.0 RCMs. Moreover, the NAR-
906 ClIM 2.0 ensemble mean reduces the overall minimum temperature bias of the CMIP6 GCM ense-
907 mble by almost half, attesting to the added value conferred by the NARClIM 2.0 RCMs with respect to
908 near-surface temperature variables.

909 Consideration of observational uncertainty is warranted. We have evaluated NARClIM RCM
910 skill via comparison with AGCD observations. Whilst AGCD are a high quality gridded observational
911 data set, like any set of observations, they contain errors and uncertainties. Consequently, the out-
912 comes of our evaluations depend on both the models being evaluated and the AGCD observational
913 dataset. This is clearly a broader issue that applies to any model evaluation versus observations. Un-
914 certainties in AGCD for temperature and precipitation arise from sparse station coverage in some lo-
915 cations, especially in remote areas, and interpolation errors in generating gridded data. More specifi-
916 cally, temperature uncertainties include urban heat island effects, inhomogeneities in observation rec-
917 ords, and elevation differences. Precipitation uncertainties involve underestimation of extremes, rain
918 gauge measurement errors, and challenges in representing complex terrain. For our purposes, the
919 question of how much of a model bias of ~ 0.5 K is due to the model errors versus the observational
920 uncertainty cannot be currently quantified, because the models are evaluated against this single obser-
921 vational dataset. This leaves the observational uncertainty as implicitly included in our results. In the
922 future observational uncertainty could be explicitly considered using a method like the Observation
923 Range Adjusted (ORA) statistics (Evans and Imran, 2024).

924 **8.3 CORDEX-CMIP6 NARClIM 2.0 climate change projections**

925 In terms of NARClIM 2.0 future climate projections, major changes between NARClIM generations
926 such as differences in GHG scenarios mean that NARClIM 2.0 projected temperature changes differ
927 in some respects to those of its predecessors. Overall, as is expected, projected warming is less intense
928 in NARClIM 2.0 under SSP3-7.0 than for NARClIM 1.5 under RCP8.5. Other differences in the pro-
929 jections between NARClIM generations require further investigation in order to explain, such as
930 NARClIM 1.5's latitudinal warming gradient for maximum temperature that contrasts with NARClIM
931 2.0's band of faster warming over central Australia relative to northern and southern regions. Irrespec-
932 tive of these differences, all three NARClIM ensembles show widespread statistically significant-
933 agreeing results for warming projections.

934 Precipitation projections for the different NARClIM generations show some key similarities,
935 such as reductions in mean annual precipitation over eastern Australia for NARClIM 2.0 and NAR-
936 ClIM 1.5, though a difference is that these are statistically significant over some areas only for NAR-
937 ClIM 1.5. The NARClIM 2.0-SSP3-7.0 and SSP1-2.6 ensembles differ in that the former generally
938 projects wet changes over northern and western Australia, whereas the latter is generally dry, results
939 that appear partially traceable to the underlying driving CMIP6-SSP data (Supporting Information
940 Figure S16).

941 Some NARClIM 2.0 RCMs produce very similar precipitation projections for certain GCM-
942 RCM combinations. Notably, ACCESS-ESM-1-5-R3 and R5 under SSP3-7.0 both produce wide-
943 spread dry projections that are substantially drier than other NARClIM 2.0 models. This GCM pro-
944 jects very dry futures across Australia (Di Virgilio et al., 2022), so this result in the R3 and R5 RCMs
945 could be largely inherited from the driving data. There are 40 realisations for ACCESS-ESM1-5, but
946 only realisation 6 provides sub-daily outputs that can be used in dynamical downscaling using WRF.
947 This realisation simulates a particularly dry projection over Australia, especially for eastern Australia,
948 making it a useful "stress test" case. In terms of GCM skill versus observations, globally, this GCM is
949 dry biased over a few regions owing to a location bias with the Inter-tropical Convergence Zone
950 (Rashid et al., 2022; Ziehn et al., 2020).

951 In other instances, there are marked divergences between the NARClIM 2.0 R3 versus R5
952 precipitation projections when forced with the same GCM. An example is UK-ESM-1-0-LL under
953 SSP3-7.0 where R3 projects stronger precipitation increases that are more geographically widespread
954 relative to R5. This raises the question of varying sources of uncertainty in the climate projections,
955 i.e., to what extent these are attributable to GCMs versus RCMs, as well as other factors.

956 **8.4 Summary**

957 In summary, the CORDEX-CMIP6 NARClIM 2.0 regional climate projections are a 10-member en-
958 semble comprising two configurations of the WRF RCM dynamically downscaling five GCMs under
959 three SSPs at 20 km resolution over CORDEX-Australasia and at 4 km convection-permitting resolu-
960 tion over south-east Australia. In addition to several high-level model design changes, e.g., increased
961 spatial resolution, a large (N=78) RCM-physics test suite is evaluated to select two new WRF RCM
962 configurations for CMIP6-forced NARClIM 2.0 climate projections. The NARClIM 2.0 physics tests
963 identified RCM configurations that generally performed well in simulating the recent Australian cli-
964 mate over southeast Australia. A key finding was that WRF RCMs using the Noah-MP LSM general-
965 ly out-performed RCMs using other LSMs in representing regional climate. Despite the overall per-
966 formance gains evident for RCMs using Noah-MP, these improvements were superior over temper-
967 ate/coastal regions of southeast Australia relative to the semi-arid interior. These performance charac-
968 teristics might be linked to Noah-MP's development being focused on Northern Hemisphere mid-
969 latitudes, including assumptions such as accounting for differences in seasonality in the Northern ver-
970 sus Southern Hemispheres by shifting the Northern Hemisphere LAI profiles by 6 months. For the
971 southeast Australian context, noting its distinctive coastal dry-sclerophyll and expansive inland grass-
972 land biomes, such assumptions might lead to discontinuities in quantities such as LAI. Given the geo-
973 graphic focus of Noah-MP's development, as well as its performance characteristics, it may be more
974 suited to application over the temperate regions of Australia rather than the semi-arid interior. It is
975 also possible that modifying/tuning Noah-MP to specific aspects of the Australian context would yield
976 performance benefits for follow-up dynamical downscaling.

977 Overall, the CMIP6-NARClIM 2.0 ensemble produces a good representation of recent mean
978 climate that in several key respects improves upon the model skill of earlier NARClIM generations.
979 This study provides a foundation for more detailed investigations of the model biases and future cli-
980 mate changes described here, including process-focused studies exploring their mechanisms.
981 CORDEX-CMIP6 NARClIM 2.0 RCM data provide valuable resources to investigate projected cli-
982 mate changes, their impacts on societies and natural systems, and potential climate change mitigation
983 and adaptation actions for the CORDEX-Australasia region.

984 **9. Code Availability**

985 A frozen version of the source code for the Weather Research and Forecasting (WRF) version 4.1.2
986 used in this study, as well as the configuration files for the simulations, is available on Zenodo at:

987 <https://doi.org/10.5281/zenodo.11184830>

988 **10. Data Availability**

989 Data for the NARClIM 2.0 CMIP6-forced R3 and R5 RCMs are being made available via [National](#)
990 [Computing Infrastructure](#) (NCI). WRF namelist settings for the NARClIM 2.0 CMIP6-forced R3 and
991 R5 RCMs are shown in Supplementary Material Figure S1 and are also available at:
992 <https://doi.org/10.5281/zenodo.11184830>. Data NARClIM 1.5 RCMs are available via the [New South](#)
993 [Wales Climate Data Portal](#) and [CORDEX-DKRZ](#). Data for NARClIM 1.0 RCMs are available via the
994 [New South Wales Climate Data Portal](#). CMIP6 GCM data are available via the [Earth System Grid](#)
995 [Federation](#).

996 **11. Author Contribution**

997 GDV and JPE designed the models and the simulations. FJ, ET, and CT setup the models and
998 conducted the model simulations with contributions from JPE, JK, JA, DC, CR, SW, YL, MER, RG
999 and JL. GDV prepared the manuscript with contributions from all co-authors.

1000 **12. Competing Interests**

1001 The authors declare that they have no conflict of interest, noting that JK is a Topic Editor of
1002 Geoscientific Model Development.

1003 **13. Funding**

1004 This research was supported by the New South Wales Department of Climate Change, Energy, the
1005 Environment and Water as part of the NARClIM 2.0 dynamical downscaling project contributing to
1006 CORDEX Australasia. Funding was provided by the NSW Climate Change Fund for NSW and
1007 Australia Regional Climate Modelling (NARClIM) Project. This research was undertaken with the
1008 assistance of resources and services from the National Computational Infrastructure (NCI), which is
1009 supported by the Australian Government.

1010 **14. References**

1011 Andrys, J., Lyons, T. J., and Kala, J.: Evaluation of a WRF ensemble using GCM boundary conditions
1012 to quantify mean and extreme climate for the southwest of Western Australia (1970–1999),
1013 International Journal of Climatology, 36, 4406–4424, <https://doi.org/10.1002/joc.4641>, 2016.
1014 Australian Bureau of Statistics.: Regional population, Online at:
1015 <https://www.abs.gov.au/statistics/people/population/regional-population/latest-release>, 2024.

1016 Bjordal, J., Storelvmo, T., Alterskjaer, K., and Carlsen, T.: Equilibrium climate sensitivity above 5
1017 degrees C plausible due to state-dependent cloud feedback, *Nat. Geosci.*, 13, 718-+,
1018 10.1038/s41561-020-00649-1, 2020.

1019 Bureau of Meteorology.: Annual climate statement 2016, 2017.

1020 Cannon, A. J. and Innocenti, S.: Projected intensification of sub-daily and daily rainfall extremes in
1021 convection-permitting climate model simulations over North America: implications for future
1022 intensity–duration–frequency curves, *Nat. Hazards Earth Syst. Sci.*, 19, 421-440,
1023 10.5194/nhess-19-421-2019, 2019.

1024 Chen, F., Liu, C. H., Dudhia, J., and Chen, M.: A sensitivity study of high-resolution regional climate
1025 simulations to three land surface models over the western United States, *Journal of*
1026 *Geophysical Research-Atmospheres*, 119, 7271-7291, 10.1002/2014jd021827, 2014a.

1027 Chen, F., Barlage, M., Tewari, M., Rasmussen, R., Jin, J. M., Lettenmaier, D., Livneh, B., Lin, C. Y.,
1028 Miguez-Macho, G., Niu, G. Y., Wen, L. J., and Yang, Z. L.: Modeling seasonal snowpack
1029 evolution in the complex terrain and forested Colorado Headwaters region: A model
1030 intercomparison study, *Journal of Geophysical Research-Atmospheres*, 119, 13795-13819,
1031 10.1002/2014jd022167, 2014b.

1032 Chou, M. D., Suarez, M. J., Liang, X. Z., and Yan, M. M. H.: A thermal infrared radiation
1033 parameterization for atmospheric studies, *NASA Tech. Memo. NASA/TM-2001-104606*, 19,
1034 68 pp. <https://ntrs.nasa.gov/citations/20010072848>, 2001.

1035 Constantinidou, K., Hadjinicolaou, P., Zittis, G., and Lelieveld, J.: Performance of Land Surface
1036 Schemes in the WRF Model for Climate Simulations over the MENA-CORDEX Domain,
1037 *Earth Systems and Environment*, 19, 10.1007/s41748-020-00187-1, 2020.

1038 Dee, D. P., Uppala, S. M., Simmons, A. J., Berrisford, P., Poli, P., Kobayashi, S., Andrae, U.,
1039 Balmaseda, M. A., Balsamo, G., Bauer, P., Bechtold, P., Beljaars, A. C. M., van de Berg, L.,
1040 Bidlot, J., Bormann, N., Delsol, C., Dragani, R., Fuentes, M., Geer, A. J., Haimberger, L.,
1041 Healy, S. B., Hersbach, H., Hólm, E. V., Isaksen, L., Kållberg, P., Köhler, M., Matricardi, M.,
1042 McNally, A. P., Monge-Sanz, B. M., Morcrette, J. J., Park, B. K., Peubey, C., de Rosnay, P.,
1043 Tavolato, C., Thépaut, J. N., and Vitart, F.: The ERA-Interim reanalysis: configuration and
1044 performance of the data assimilation system, *Quarterly Journal of the Royal Meteorological*
1045 *Society*, 137, 553-597, 10.1002/qj.828, 2011.

1046 Di Virgilio, G., Evans, J. P., Di Luca, A., Olson, R., Argüeso, D., Kala, J., Andrys, J., Hoffmann, P.,
1047 Katzfey, J. J., and Rockel, B.: Evaluating reanalysis-driven CORDEX regional climate
1048 models over Australia: model performance and errors, *Clim. Dyn.*, 53, 2985-3005,
1049 10.1007/s00382-019-04672-w, 2019.

1050 Di Virgilio, G., Ji, F., Tam, E., Nishant, N., Evans, J. P., Thomas, C., Riley, M. L., Beyer, K., Grose,
1051 M. R., Narsey, S., and Delage, F.: Selecting CMIP6 GCMs for CORDEX Dynamical

1052 Downscaling: Model Performance, Independence, and Climate Change Signals, *Earth's*
1053 *Future*, 10, e2021EF002625, <https://doi.org/10.1029/2021EF002625>, 2022.

1054 Di Virgilio, G., Ji, F., Tam, E., Evans, J. P., Kala, J., Andrys, J., Thomas, C., Choudhury, D., Rocha,
1055 C., Li, Y., Riley, M.: Evaluation of CORDEX ERA5-forced ‘NARClIM2. 0’ regional climate
1056 models over Australia using the Weather Research and Forecasting (WRF) model version
1057 4.1.2, Geoscientific Model Development, <https://doi.org/10.5194/gmd-2024-41>, In review.

1058 DWER.: Climate Adaptation Strategy - Building WA's Climate Resilient Future, Government of
1059 Western Australia, 25 pages. Online at: [https://www.wa.gov.au/system/files/2023-](https://www.wa.gov.au/system/files/2023-07/climate_adaption_strategy_220623.pdf)
1060 [07/climate_adaption_strategy_220623.pdf](https://www.wa.gov.au/system/files/2023-07/climate_adaption_strategy_220623.pdf), 2023.

1061 Evans, A., Jones, D., Lellyett, S., and Smalley, R.: An Enhanced Gridded Rainfall Analysis Scheme
1062 for Australia, Australian Bureau of Meteorology 2020a.

1063 Evans, J. P. and Imran, H. M.: The observation range adjusted method: a novel approach to
1064 accounting for observation uncertainty in model evaluation, *Environmental Research*
1065 *Communications*, 6, 071001, 10.1088/2515-7620/ad5ad8, 2024.

1066 Evans, J. P., Ji, F., Lee, C., Smith, P., Argüeso, D., and Fita, L.: Design of a regional climate
1067 modelling projection ensemble experiment - NARClIM, *Geosci. Model Dev.*, 7, 621-629,
1068 10.5194/gmd-7-621-2014, 2014.

1069 Evans, J. P., Di Virgilio, G., Hirsch, A. L., Hoffmann, P., Remedio, A. R., Ji, F., Rockel, B., and
1070 Coppola, E.: The CORDEX-Australasia ensemble: evaluation and future projections, *Clim.*
1071 *Dyn.*, 10.1007/s00382-020-05459-0, 2020b.

1072 Fiddes, S., Pepler, A., Saunders, K., and Hope, P.: Redefining southern Australia’s climatic regions
1073 and seasons, *J. South Hemisph. Earth Syst. Sci.*, 71, 92-109, <https://doi.org/10.1071/ES20003>,
1074 2021.

1075 Giorgi, F.: Thirty Years of Regional Climate Modeling: Where Are We and Where Are We Going
1076 next?, *Journal of Geophysical Research: Atmospheres*, 124, 5696-5723,
1077 10.1029/2018jd030094, 2019.

1078 Glotfelty, T., Ramírez-Mejía, D., Bowden, J., Ghilardi, A., and West, J. J.: Limitations of WRF land
1079 surface models for simulating land use and land cover change in Sub-Saharan Africa and
1080 development of an improved model (CLM-AF v. 1.0), *Geosci. Model Dev.*, 14, 3215-3249,
1081 10.5194/gmd-14-3215-2021, 2021.

1082 Grose, M., Narsey, S., Trancoso, R., Mackallah, C., Delage, F., Dowdy, A., Di Virgilio, G.,
1083 Watterson, I., Dobrohotoff, P., Rashid, H. A., Rauniyar, S., Henley, B., Thatcher, M., Syktus,
1084 J., Abramowitz, G., Evans, J. P., Su, C.-H., and Takbash, A.: A CMIP6-based multi-model
1085 downscaling ensemble to underpin climate change services in Australia, *Climate Services*, 30,
1086 100368, <https://doi.org/10.1016/j.cliser.2023.100368>, 2023.

1087 Grose, M. R., Foster, S., Risbey, J. S., Osbrough, S., and Wilson, L.: Using indices of atmospheric
1088 circulation to refine southern Australian winter rainfall climate projections, *Clim. Dyn.*,
1089 10.1007/s00382-019-04880-4, 2019.

1090 Grose, M. R., Narsey, S., Delage, F., Dowdy, A. J., Bador, M., Boschat, G., Chung, C., Kajtar, J.,
1091 Rauniyar, S., Freund, M., Lyu, K., Rashid, H. A., Zhang, X., Wales, S., Trenham, C.,
1092 Holbrook, N. J., Cowan, T., Alexander, L. V., Arblaster, J. M., and Power, S. B.: Insights
1093 from CMIP6 for Australia's future climate, *Earth's Future*, 8, e2019EF001469,
1094 <https://doi.org/10.1029/2019EF001469>, 2020.

1095 Herger, N., Abramowitz, G., Knutti, R., Angéllil, O., Lehmann, K., and Sanderson, B. M.: Selecting a
1096 climate model subset to optimise key ensemble properties, *Earth Syst. Dynam.*, 9, 135-151,
1097 10.5194/esd-9-135-2018, 2018.

1098 Hong, S.-Y., Noh, Y., and Dudhia, J.: A New Vertical Diffusion Package with an Explicit Treatment
1099 of Entrainment Processes, *Monthly Weather Review*, 134, 2318-2341,
1100 <https://doi.org/10.1175/MWR3199.1>, 2006.

1101 Hong, S. Y. and Lim, J.-O. J.: The WRF Single-Moment 6-Class Microphysics Scheme (WSM6),
1102 *Asia-Pac. J. Atmos. Sci.*, 42, 129-151, 2006.

1103 Hsiang, S., Kopp, R., Jina, A., Rising, J., Delgado, M., Mohan, S., Rasmussen, D. J., Muir-Wood, R.,
1104 Wilson, P., Oppenheimer, M., Larsen, K., and Houser, T.: Estimating economic damage from
1105 climate change in the United States, *Science*, 356, 1362-1368, 10.1126/science.aal4369, 2017.

1106 Huang, Y., Xue, M., Hu, X.-M., Martin, E., Novoa, H. M., McPherson, R. A., Perez, A., and Morales,
1107 I. Y.: Convection-Permitting Simulations of Precipitation over the Peruvian Central Andes:
1108 Strong Sensitivity to Planetary Boundary Layer Parameterization, *J. Hydrometeorol.*, 24,
1109 1969-1990, <https://doi.org/10.1175/JHM-D-22-0173.1>, 2023.

1110 Iacono, M. J., Delamere, J. S., Mlawer, E. J., Shephard, M. W., Clough, S. A., and Collins, W. D.:
1111 Radiative forcing by long-lived greenhouse gases: Calculations with the AER radiative
1112 transfer models, *Journal of Geophysical Research: Atmospheres*, 113,
1113 <https://doi.org/10.1029/2008JD009944>, 2008.

1114 Imran, H. M., Kala, J., Ng, A. W. M., and Muthukumaran, S.: An evaluation of the performance of a
1115 WRF multi-physics ensemble for heatwave events over the city of Melbourne in southeast
1116 Australia, *Clim. Dyn.*, 50, 2553-2586, 10.1007/s00382-017-3758-y, 2018.

1117 IPCC: *Climate Change 2021: The Physical Science Basis. Contribution of Working Group I to the*
1118 *Sixth Assessment Report of the Intergovernmental Panel on Climate Change*, Cambridge
1119 University Press, 2021.

1120 Iturbide, M., Gutiérrez, J. M., Alves, L. M., Bedia, J., Cerezo-Mota, R., Cimadevilla, E., Cofiño, A.
1121 S., Di Luca, A., Faria, S. H., Gorodetskaya, I. V., Hauser, M., Herrera, S., Hennessy, K.,
1122 Hewitt, H. T., Jones, R. G., Krakovska, S., Manzanas, R., Martínez-Castro, D., Narisma, G.
1123 T., Nurhati, I. S., Pinto, I., Seneviratne, S. I., van den Hurk, B., and Vera, C. S.: An update of

1124 IPCC climate reference regions for subcontinental analysis of climate model data: definition
1125 and aggregated datasets, *Earth Syst. Sci. Data*, 12, 2959-2970, 10.5194/essd-12-2959-2020,
1126 2020.

1127 Janjić, Z. I.: Comments on “Development and Evaluation of a Convection Scheme for Use in Climate
1128 Models”, *Journal of the Atmospheric Sciences*, 57, 3686-3686, [https://doi.org/10.1175/1520-
1129 0469\(2000\)057<3686:CODAEO>2.0.CO;2](https://doi.org/10.1175/1520-0469(2000)057<3686:CODAEO>2.0.CO;2), 2000.

1130 Kain, J. S.: The Kain-Fritsch convective parameterization: An update, *Journal of Applied
1131 Meteorology*, 43, 170-181, 10.1175/1520-0450(2004)043<0170:tkcpau>2.0.co;2, 2004.

1132 Kendon, E. J., Prein, A. F., Senior, C. A., and Stirling, A.: Challenges and outlook for convection-
1133 permitting climate modelling, *Philosophical transactions. Series A, Mathematical, physical,
1134 and engineering sciences*, 379, 20190547, 10.1098/rsta.2019.0547, 2021.

1135 Kendon, E. J., Ban, N., Roberts, N. M., Fowler, H. J., Roberts, M. J., Chan, S. C., Evans, J. P., Fosser,
1136 G., and Wilkinson, J. M.: Do convection-permitting regional climate models improve
1137 projections of future precipitation change?, *Bulletin of the American Meteorological Society*,
1138 98, 79-+, 10.1175/bams-d-15-0004.1, 2017.

1139 King, A. D., Alexander, L. V., and Donat, M. G.: The efficacy of using gridded data to examine
1140 extreme rainfall characteristics: a case study for Australia, *International Journal of
1141 Climatology*, 33, 2376-2387, 10.1002/joc.3588, 2013.

1142 Kusaka, H. and Kimura, F.: Coupling a Single-Layer Urban Canopy Model with a Simple
1143 Atmospheric Model: Impact on Urban Heat Island Simulation for an Idealized Case, *Journal
1144 of the Meteorological Society of Japan. Ser. II*, 82, 67-80, 10.2151/jmsj.82.67, 2004.

1145 Lee, D., Min, S.-K., Ahn, J.-B., Cha, D.-H., Shin, S.-W., Chang, E.-C., Suh, M.-S., Byun, Y.-H., and
1146 Kim, J.-U.: Uncertainty analysis of future summer monsoon duration and area over East Asia
1147 using a multi-GCM/multi-RCM ensemble, *Environ. Res. Lett.*, 18, 064026, 10.1088/1748-
1148 9326/acd208, 2023.

1149 Lucas-Picher, P., Argüeso, D., Brisson, E., Trambly, Y., Berg, P., Lemonsu, A., Kotlarski, S., and
1150 Caillaud, C.: Convection-permitting modeling with regional climate models: Latest
1151 developments and next steps, *WIREs Climate Change*, 12, e731,
1152 <https://doi.org/10.1002/wcc.731>, 2021.

1153 Meehl, G. A., Senior, C. A., Eyring, V., Flato, G., Lamarque, J.-F., Stouffer, R. J., Taylor, K. E., and
1154 Schlund, M.: Context for interpreting equilibrium climate sensitivity and transient climate
1155 response from the CMIP6 Earth system models, *Science Advances*, 6, eaba1981,
1156 10.1126/sciadv.aba1981, 2020.

1157 Murphy, B. F. and Timbal, B.: A review of recent climate variability and climate change in
1158 southeastern Australia, *International Journal of Climatology*, 28, 859-879,
1159 <https://doi.org/10.1002/joc.1627>, 2008.

1160 Nakanishi, M. and Niino, H.: Development of an Improved Turbulence Closure Model for the
1161 Atmospheric Boundary Layer, *Journal of the Meteorological Society of Japan. Ser. II*, 87,
1162 895-912, 10.2151/jmsj.87.895, 2009.

1163 Nishant, N., Evans, J. P., Di Virgilio, G., Downes, S. M., Ji, F., Cheung, K. K. W., Tam, E., Miller, J.,
1164 Beyer, K., and Riley, M. L.: Introducing NARClIM1.5: Evaluating the Performance of
1165 Regional Climate Projections for Southeast Australia for 1950–2100, *Earth's Future*, 9,
1166 e2020EF001833, <https://doi.org/10.1029/2020EF001833>, 2021.

1167 Niu, G.-Y., Yang, Z.-L., Mitchell, K. E., Chen, F., Ek, M. B., Barlage, M., Kumar, A., Manning, K.,
1168 Niyogi, D., Rosero, E., Tewari, M., and Xia, Y.: The community Noah land surface model
1169 with multiparameterization options (Noah-MP): 1. Model description and evaluation with
1170 local-scale measurements, *Journal of Geophysical Research: Atmospheres*, 116,
1171 10.1029/2010jd015139, 2011.

1172 NSW Government.: NSW Climate Change Fund Annual Report 2021-22, 2022.

1173 NSW Government.: NSW Climate Change Fund Annual Report 2022-23, 2023.

1174 Nuryanto, D. E., Satyaningsih, R., Nuraini, T. A., Rizal, J., Heriyanto, E., Linarka, U. A., and
1175 Sopaheluwakan, A.: Evaluation of Planetary Boundary Layer (PBL) schemes in simulating
1176 heavy rainfall events over Central Java using high resolution WRF model, *Sixth International
1177 Symposium on LAPAN-IPB Satellite, SPIE*, 2019.

1178 Oleson, K., Lawrence, D., Bonan, G. B., Flanner, M., Kluzek, E., Lawrence, P., Levis, S., Swenson,
1179 S. C., Thornton, P. E., Dai, A., Decker, M., Dickinson, R., Feddema, J., Heald, C., Hoffman,
1180 F., Lamarque, J.-F., Mahowald, N., Niu, G.-Y., Qian, T., and Zeng, X.: Technical Description
1181 of version 4.0 of the Community Land Model (CLM), 2010.

1182 Pepler, A. and Dowdy, A.: Intense east coast lows and associated rainfall in eastern Australia, *J. South
1183 Hemisph. Earth Syst. Sci.*, 71, 110-122, 10.1071/es20013, 2021.

1184 Perkins, S. E., Pitman, A. J., Holbrook, N. J., and McAneney, J.: Evaluation of the AR4 climate
1185 models' simulated daily maximum temperature, minimum temperature, and precipitation over
1186 Australia using probability density functions, *J. Clim.*, 20, 4356-4376, 10.1175/jcli4253.1,
1187 2007.

1188 Pleim, J. E.: A Combined Local and Nonlocal Closure Model for the Atmospheric Boundary Layer.
1189 Part I: Model Description and Testing, *J. Appl. Meteorol. Climatol.*, 46, 1383-1395,
1190 <https://doi.org/10.1175/JAM2539.1>, 2007.

1191 Rashid, H. A., Sullivan, A., Dix, M., Bi, D., Mackallah, C., Ziehn, T., Dobrohotoff, P., O'Farrell, S.,
1192 Harman, I. N., Bodman, R., and Marsland, S.: Evaluation of climate variability and change in
1193 ACCESS historical simulations for CMIP6, *J. South Hemisph. Earth Syst. Sci.*, 72, 73-92,
1194 <https://doi.org/10.1071/ES21028>, 2022.

1195 Salamanca, F., Zhang, Y. Z., Barlage, M., Chen, F., Mahalov, A., and Miao, S. G.: Evaluation of the
1196 WRF-Urban Modeling System Coupled to Noah and Noah-MP Land Surface Models Over a

1197 Semiarid Urban Environment, *Journal of Geophysical Research-Atmospheres*, 123, 2387-
1198 2408, 10.1002/2018jd028377, 2018.

1199 Sherwood, S. C., Webb, M. J., Annan, J. D., Armour, K. C., Forster, P. M., Hargreaves, J. C., Hegerl,
1200 G., Klein, S. A., Marvel, K. D., Rohling, E. J., Watanabe, M., Andrews, T., Braconnot, P.,
1201 Bretherton, C. S., Foster, G. L., Hausfather, Z., von der Heydt, A. S., Knutti, R., Mauritsen,
1202 T., Norris, J. R., Proistosescu, C., Rugenstein, M., Schmidt, G. A., Tokarska, K. B., and
1203 Zelinka, M. D.: An Assessment of Earth's Climate Sensitivity Using Multiple Lines of
1204 Evidence, *Rev. Geophys.*, 58, e2019RG000678, <https://doi.org/10.1029/2019RG000678>,
1205 2020.

1206 Skamarock, W. C., Klemp, J. B., Dudhia, J., Gill, D. O., Barker, D. M., Wang, W., and Powers, J. G.:
1207 A description of the Advanced Research WRF Version 3. NCAR Tech Note NCAR/TN-
1208 475+STR. NCAR, Boulder, CO, 2008.

1209 Tegen, I., Hollrig, P., Chin, M., Fung, I., Jacob, D., and Penner, J.: Contribution of different aerosol
1210 species to the global aerosol extinction optical thickness: Estimates from model results,
1211 *Journal of Geophysical Research: Atmospheres*, 102, 23895-23915,
1212 <https://doi.org/10.1029/97JD01864>, 1997.

1213 Tewari, M., Wang, W., Dudhia, J., LeMone, M. A., Mitchell, K., Ek, M., Gayno, G., Wegiel, J., and
1214 Cuenca, R.: Implementation and verification of the united NOAH land surface model in the
1215 WRF model, 11-15 pp.2016.

1216 Thompson, G., Field, P. R., Rasmussen, R. M., and Hall, W. D.: Explicit Forecasts of Winter
1217 Precipitation Using an Improved Bulk Microphysics Scheme. Part II: Implementation of a
1218 New Snow Parameterization, *Monthly Weather Review*, 136, 5095-5115,
1219 <https://doi.org/10.1175/2008MWR2387.1>, 2008.

1220 Tiedtke, M.: A Comprehensive Mass Flux Scheme for Cumulus Parameterization in Large-Scale
1221 Models, *Monthly Weather Review*, 117, 1779-1800, 10.1175/1520-
1222 0493(1989)117<1779:acmfsf>2.0.co;2, 1989.

1223 Torma, C., Giorgi, F., and Coppola, E.: Added value of regional climate modeling over areas
1224 characterized by complex terrain—Precipitation over the Alps, *Journal of Geophysical*
1225 *Research: Atmospheres*, 120, 3957-3972, 10.1002/2014JD022781, 2015.

1226 WCRP: CORDEX experiment design for dynamical downscaling of CMIP6 (DRAFT),
1227 [https://cordex.org/wp-content/uploads/2020/06/CORDEX-](https://cordex.org/wp-content/uploads/2020/06/CORDEX-CMIP6_exp_design_draft_20200610.pdf)
1228 [CMIP6_exp_design_draft_20200610.pdf](https://cordex.org/wp-content/uploads/2020/06/CORDEX-CMIP6_exp_design_draft_20200610.pdf), 2020.

1229 WCRP: CORDEX-CMIP6 Data Request, Coordinated Regional Downscaling Experiment
1230 (CORDEX), [https://cordex.org/wp-content/uploads/2022/03/CORDEX-](https://cordex.org/wp-content/uploads/2022/03/CORDEX-CMIP6_Data_Request_tutorial.pdf)
1231 [CMIP6_Data_Request_tutorial.pdf](https://cordex.org/wp-content/uploads/2022/03/CORDEX-CMIP6_Data_Request_tutorial.pdf), 2022.

1232 Whetton, P. and Hennessy, K.: Potential benefits of a “storyline” approach to the provision of regional
1233 climate projection information, International Climate Change Adaptation Conference,
1234 NCARF, Gold Coast, Australia, 2010.

1235 Wilks, D. S.: “The Stippling Shows Statistically Significant Grid Points”: How Research Results are
1236 Routinely Overstated and Overinterpreted, and What to Do about It, Bulletin of the American
1237 Meteorological Society, 97, 2263-2273, <https://doi.org/10.1175/BAMS-D-15-00267.1>, 2016.

1238 Xie, K., Li, L., Chen, H., Mayer, S., Dobler, A., Xu, C. Y., and Gokturk, O. M.: Enhanced Evaluation
1239 of Sub-daily and Daily Extreme Precipitation in Norway from Convection-Permitting Models
1240 at Regional and Local Scales, Hydrol. Earth Syst. Sci. Discuss., 2024, 1-38, 10.5194/hess-
1241 2024-68, 2024.

1242 Zhuo, L., Dai, Q., Han, D., Chen, N., and Zhao, B.: Assessment of simulated soil moisture from WRF
1243 Noah, Noah-MP, and CLM land surface schemes for landslide hazard application, Hydrol.
1244 Earth Syst. Sci., 23, 4199-4218, 10.5194/hess-23-4199-2019, 2019.

1245 Ziehn, T., Chamberlain, M. A., Law, R. M., Lenton, A., Bodman, R. W., Dix, M., Stevens, L., Wang,
1246 Y.-P., and Srbinovsky, J.: The Australian Earth System Model: ACCESS-ESM1.5, J. South
1247 Hemisph. Earth Syst. Sci., 70, 193-214, <https://doi.org/10.1071/ES19035>, 2020.